APPLICATION OF ANTI-LRP/LR SPECIFIC ANTIBODIES ON NEOPLASTIC CELL LINES FOR METASTATIC CANCER TREATMENT

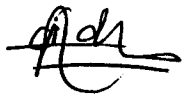
Aadilah Omar

A dissertation submitted to the Faculty of Science, University of the Witwatersrand, in fulfillment of the requirements for the degree Master of Science

Johannesburg, 2012

DECLARATION

I declare that this Dissertation is my own, unaided work. It is being submitted for the Degree of Master of Science at the University of the Witwatersrand, Johannesburg. It has not been submitted before for any degree or examination at any other University.



_____

14th day of May 2012

ABSTRACT

The 37kDa/67kDa laminin receptor (LRP/LR) is thought to play a major role in the adhesion to laminin and consequently invasion resulting in the metastasis of tumor cells. This receptor is reported to be over-expressed in several neoplastic cell lines and is believed to increase tumor aggressiveness. This research aims at determining whether the application of anti-LRP/LR specific antibody (IgG1-iS18) on neoplastic cell lines would result in a decrease in invasion and adhesion. All neoplastic cell lines had significantly increased cell surface LRP/LR levels compared to NIH/3T3 cells, with the most notable increase seen in SW480 cells (10.98%). Due to a positive correlation between the cell surface LRP/LR levels and invasion potential we propose that an increased LRP/LR level correlates to an increased ability to invade. A significantly decreased adhesion potential was noted in all neoplastic cell lines except the non-invasive MCF-7 cell line, upon application of IgG1-iS18, 21% decrease in HT-1080 cells, 14% in HeLa, 20% in LNCaP, 48% and 74% in A549 and SW480 cells, respectively. Incubation with the anti-LRP/LR antibody IgG1-iS18 resulted in a significant reduction of the invasive potential of HT-1080 (44%), A549 (33%), HeLa (69%), SW480 (91%) and LNCaP cells (38%). Furthermore, a high Pearson's correlation coefficient between adhesion potential and invasive potential was seen, confirming that adhesion is indeed a pre-requisite for invasion. The significant reduction in invasion and adhesion of HT-1080, A549, HeLa, SW480 and LNCaP cells upon application of the IgG1-iS18 antibody suggests that this macromolecule might act as a promising therapeutic tool for the treatment of various metastatic cancer types.

ACKNOWLEDGEMENTS

I would like to thank Prof. S. F. T. Weiss for giving me this wonderful opportunity and also for all his advice, guidance and time, ensuring that my project was a success and my results submitted for publication.

For financial aid, I would like to acknowledge the University of the Witwatersrand for the Postgraduate Merit Award Scholarship and the National Research Foundation of South Africa for the Prestigious and Equity Scholarship.

Antibody was kindly supplied by Affimed Therapeutics, Heidelburg, Germany.

A special thanks to all the members of the Weiss laboratory, Dr. Vusi Mbazima whose assistance was invaluable. My lovely ladies Bianca Da Costa Dias, Kianshanee Moodley, Danielle Gonsalves and Raksha Khusal, who I will always share fond memories with and made time in the laboratory and the study room amazing and fun!

Words cannot describe my appreciation for the support and motivation I received from my dearest friend Katarina Jovanovic who always had faith in me. Without your help this work would not have been possible, your optimism and inspiration kept me going and I will always be grateful for this.

Last but not least I would like to thank my parents for all the prayers and for cheering me on, and my partner and best friend Zaheer ‘Boo’ Abdulla ☺ for his words of encouragement. Love you lots!

RESEARCH OUTPUT

1. Original publications:

- Omar A, Reusch U, Knackmuss S, Little M and Weiss S. F. T. (2012). Anti-LRP/LR specific antibody IgG1-iS18 significantly reduces adhesion and invasion of metastatic lung, cervix, colon and prostate cells. *Journal of Molecular Biology* **419:** 102-109.

- Kolodziejczak D, Da Costa Dias B, Zuber C, Jovanovic K, Omar A, Beck J, Vana K, Mbazima V, Richt J, Brenig B and Weiss S. F. T. (2010). Prion Interaction with the 37-kDa/67-kDa Laminin Receptor on Enterocytes as a Cellular Model for Intestinal Uptake of Prions. *Journal of Molecular Biology* **402**: 293-300.

2. Reviews:

- Omar A, Jovanovic K, Da Costa Dias B, Gonsalves D, Moodley K, Caveny R, Mbazima V and Weiss S. F. T. (2011). Patented biological approaches for the therapeutic modulation of the 37kDa/67kDa laminin receptor. *Expert Opinion on Therapeutic Patents* **21**(1):35-53.

- Mbazima V, Da Costa Dias B, Omar A, Jovanovic K and Weiss S. F. T. (2010). Interactions between PrP(c) and other ligands with the 37-kDa/67-kDa laminin receptor. *Frontiers in Biosciences* **15:** 1150-1163.

3. Conference contributions:

Poster presentations

- Omar A, Moodley K, Khusal R and Weiss S. F. T. Anti-LRP/LR specific antibodies significantly reduces cell adhesion and cell viability of various metastatic cancer types. Cell and Developmental Biology Mini Symposium at The University of the Witwatersrand Medical School, 22 May 2011.

- Omar A, Knackmuss S, Reusch U, Little M and Weiss S. F . T. Anti-LRP/LR specific antibody IgG1-iS18 significantly reduced cell adhesion and cell invasion of various metastatic cancer types. Molecular Biology Research Thrust (MBRT) conference at The University of the Witwatersrand Postgraduate Development Hub, 7 December 2011.

- Omar A, Knackmuss S, Reusch U, Little M and Weiss S. F . T. Anti-LRP/LR specific antibody IgG1-iS18 significantly reduced cell adhesion and cell invasion of various metastatic cancer types.South African Society of Biochemistry and Molecular Biology Congress at Champagne Sports Resort, Drakensberg, KwaZulu-Natal, 29 January 2012.

LIST OF FIGURES

Figure 1:	Percentage of deaths attributed to cancer	2
Figure 2:	Comparison of normal and tumour cell division/proliferation	4
Figure 3:	The 37kDa Laminin Receptor Precursor molecule	5
Figure 4:	Illustration of the process of metastasis	8
Figure 5:	Electron micrograph of HT-1080 cell migration	8
Figure 6:	Schematic diagram illustrating cell invasion	9
Figure 7:	Illustration of a full length Immunoglobulin	10
Figure 8:	Principle of invasion assay	27
Figure 9:	Principle of adhesion assay	29
Figure 10:	Principle of semi-dry Transfer Western Blotting method	31
Figure 11:	Immuno-detection of proteins	32
Figure 12:	Biochemical analysis of antibodies that were over-expressed	34
Figure 13:	Western Blot detection 37kDa LRP using antibody produced	35
Figure 14:	Detection of 37kDa LRP on surface of cell lines	37
Figure 15:	Bar chart of surface LRP levels	38
Figure 16:	Western Blot of total LRP levels	39
Figure 17:	Bar chart of total LRP levels	40
Figure 18:	Bar chart of adhesion assay results	42
Figure 19:	Bar chart of neoplastic cell lines invasive potential	44
Figure 20:	Bar chart of effect of antibodies on HT-1080 cells	46
Figure 21:	Bar chart of effect of antibodies on HeLa cells	46
Figure 22:	Bar chart of effect of antibodies on A549 cells	47
Figure 23:	Bar chart of effect of antibodies on LNCaP cells	47
Figure 24:	Bar chart of effect of antibodies on SW480 cells	48
Figure 25:	Representative photographs of invasion assay results	49

LIST OF TABLES

Table 1:	Characterization of cancer stages	3
Table 2:	Currently available monoclonal antibodies for cancer treatment	12
Table 3:	Bacterial strains used in antibody production	15
Table 4:	Cell lines used for *in vitro* experiments	16
Table 5:	Storage solutions used for freezing cell lines	17
Table 6:	Solutions used in SDS-PAGE	20
Table 7:	Solutions used in Western Blotting	20
Table 8:	Solutions used in IgG purification	21
Table 9:	Antibodies used in the various experiments	21
Table 10:	Percentage reduction in adhesion potential	42
Table 11:	Tumorigenic cell lines invasive behavior and potential	44
Table 12:	Summary of invasion assay results	48
Table 13:	Pearson's correlation coefficient values	53

ABBREVIATIONS

aa	Amino acid
AAV	Adeno associated virus
ADC's	Antibody drug conjugates
APS	Ammonium peroxisulfate
BCA	Bicinchonic acid
C-terminus	Carboxy terminus
CTLA-4	Cytotoxic T-lymphocyte Antigen 4
DPBS	Dulbecco's phosphate buffer solution
DMEM	Dulbecco's modified eagle media
DMSO	Dimethyl sulfoxide
DNA	Deoxyribonucleic acid
DOC	Deoxycholic acid
DTT	Dithioreitol
E.R	Endoplastic reticulum
EBV	Ebstein Barr Virus
EBNA	Ebstein Barr nuclear antigen
ECM	Extracellular matrix
EDTA	Ethylenediaminetetracetic acid
EHS	Engelbreth-Holm-Swarm
EpCAM	Epithelial cell adhesion molecule
ErbB2	Erythroblastic leukemia viral oncogene homolog 2
FACS	Fluorescent activated cell scanning
FCS	Fetal calf serum
FITC	Fluorescein isothiocynate
HC	Heavy chain
Hep3B	Human hepatoma cells
HEPES	4-(2-hydroxyethyl)-1-piperazineethanesulfonic acid
HM2602	Heparan sulfate mimetic 2602
HRP	Horse radish peroxidase
IgG	Immunoglobulin
IgG1-iS18	Immunoglobulin G 1 iS18
IOD	Integrated optical density

ITS	Insulin transferrin selenium
LB	Luria bertani
LC	Light chain
LRP	Laminin receptor precursor
LR	Laminin receptor
MAb's	Monoclonal antibodies
MAPK	Mitogen activated protein kinase
MMP	Matrix metalloproteinase
MRI	Magnetic resonance imaging
MWCO	Molecular weight cut-off
N-terminus	Amino terminus
P4G	Anti-LRP antibody
p53	Tumor protein 53
PBS	Phostphate buffered saline
PFA	Paraformaldehyde
POD	Peroxidase
PVDF	Polyvinylidene fluoride
RNA	Ribonucleic acid
RPMI 1640	Roswell Park Memorial Institute media
ScFv IgG	Single chain variable fragment immunoglobulin G
SDS	Sodium dodecylsulfate
SDS-PAGE	Sodium dodecylsulfate polyacrylamide gel electrophoresis
siRNA	Single interfering ribonucleic acid
SP-54	Pentosan sulfate 54
TC	Tissue culture
TE	Tris EDTA
TEMED	N, N, N', N' - tetramethylethylenediamine
TGF-ß	Transforming growth factor ß
VEE	Venezuelan equine encephalitis virus
VEGF	Vascular endothelial growth factor

CONTENTS PAGE

DECLARATION II

ABSTRACT III

ACKNOWLEDGEMENTS IV

RESEARCH OUTPUT V

LIST OF FIGURES VI

LIST OF TABLES VII

ABBREVIATIONS VIII

CHAPTER ONE – INTRODUCTION 1

1.1 Cancer 1

1.2 Classification of cancer 2

1.3 Progression of cancer 3

1.4 Laminin 4

1.5 LRP/LR 5

1.6 The 37kDa/67kDa LRP/LR and cancer 6

1.7 Antibodies 10

1.8 Therapeutic antibodies 11

1.9 Anti-LRP/LR specific antibody IgG1-iS18 13

1. 10 Aims and objectives 14

CHAPTER TWO – MATERIALS 15

2.1. Molecular biology 15
2.1.1 Plasmids 15
2.1.2 Bacterial strains 15

2.2 Cell culture 16
2.2.1 Eukaryotic cell lines 16
2.2.2 Cell culture media 16
2.2.3 Cell culture material 18
2.2.4 Material for cell lysates 18
2.2.5 Material for transient transfection 18
2.2.6 Material for invasion and adhesion assays 19

2.3 Protein biochemistry **20**
2.3.1. Solutions and reagents 20
2.3.2. Antibodies 21

CHAPTER THREE – METHODS **22**

3.1. Molecular biology **22**
3.1.1 Plasmid DNA isolation 22

3.2. Cell culture **22**
3.2.1 Cell cultivation 22
3.2.2 Freezing and thawing of cells 22
3.2.3 Cell count determination 23
3.2.4 Preparation of cell lysates 23
3.2.5 BCA™ protein assay 23

3.3 Antibody production **24**
3.3.1 Synthesis of IgG1-iS18 and IgG1-HD37 in mammalian cells 24
3.3.2 Purification of IgG1-iS18 and –HD37 by protein A sepharose affinity chromatography 24
3.3.3 Dialysis of IgG1-iS18 and IgG1-HD37 25
3.3.4 Detection of IgG1-iS18 and IgG1-HD37 25
3.3.5 Quantification of IgG1-iS18 and IgG1-HD37 25

3.4 FACS (Fluorescence activated cell scanning) **26**

3.5 Invasion assays **27**
3.5.1 Preparation of Transwell inserts, cells and determination of invasive potential 28

3.6 Adhesion assay **29**

3.7 Protein Biochemistry **30**
3.7.1 Sodium dodecyl sulfate polyacrylamide gel electrophoresis (SDS-PAGE) 30
3.7.2 Western Blotting 30
3.7.3 Protein detection and chemiluminescence 31

3.8 Data analysis and statistical evaluation **32**

CHAPTER FOUR – RESULTS **33**

4.1 Production of anti-LRP/LR specific antibody IgG1-iS18 in mammalian cells **33**
4.1.1 Characterization of the plasmids 33
4.1.2 Antibody over-expression in HEK293 EBNA cells 33
4.1.3 Purification and detection of IgG1-iS18 and IgG1-HD37 34
4.1.4 Dialysis of IgG1-iS18 and IgG1-HD37 35
4.1.5 Characterization of IgG1-iS18 35

4.2 LRP levels **36**
4.2.1 Cell surface LRP levels 36
4.2.2 Total LRP levels 39

4.3 Cell adhesion potential **41**

4.4 Invasive potential **43**
4.4.1 Determination of cell invasive potential of selected neoplastic cell lines 43
4.4.2 IgG1-iS18 significantly decreased the invasive potential in neoplastic cell lines 45

CHAPTER FIVE – DISCUSSION **50**

5.1 Antibody development **50**

5.2 Process of metastasis **51**

5.3 LRP/LR, cell surface LRP and total LRP levels **51**

5.4 Surface and total LRP levels appear not to be an accurate indication of invasive potential **53**

5.5 Optimizing invasion assay **53**

5.6 Effect of IgG1-iS18 antibody on invasion and adhesion **54**

5.7 Antibody activity **55**

5.8 Outlook **55**

6. REFERENCES **57**

7. APPENDIX **62**

CHAPTER ONE – INTRODUCTION

1.1 Cancer

Cancer is one of the leading causes of mortality globally and was found to be responsible for approximately 13% of all deaths worldwide in 2007 (http://www.who.int/cancer/en/. Retrieved March 4, 2010). Predictions have shown an increased mortality rate resulting from this disease with an estimated 12 million deaths by 2030 (http://www.who.int/cancer/en/. Retrieved March 4, 2010). The most striking feature of this disease is that it affects people of all ages, races, genders and economic statuses. According to the World Health Organization the most frequent cancer types that occur in both sexes worldwide are, in order of decreasing incidence rate, breast cancer, prostate cancer, lung cancer, colorectal cancer and cervix uteri cancer (GLOBOCAN 2008 (IARC)). The most common cancer types occurring in the Western World include lung, breast, prostate and colon cancers (http://info.cancerresearchuk.org. Retrieved March 4, 2010). However, this differs with newly industrialized countries where the prominent cancer types include cervix and stomach cancer (Figure 1). This variance is due to progress in diagnostic techniques, which is often unaffordable to those in poorer regions. Early diagnosis is possible with the help of techniques such as magnetic resonance imaging (MRI) and leads to an overall decrease in mortality. Another aspect that plays an influential role in reducing the number of fatalities includes the discovery, and consequently, the spread of awareness regarding risk factors for cancer. Currently, several modes of treatment are available such as surgery, chemotherapy, radiation therapy, immunotherapy and monoclonal antibody therapy. Other novel approaches include gene therapy[1], non-pathogenic bacteria and telomerase therapy[2]. In cases when the tumor becomes metastatic, treatment becomes challenging since various tissues are affected.

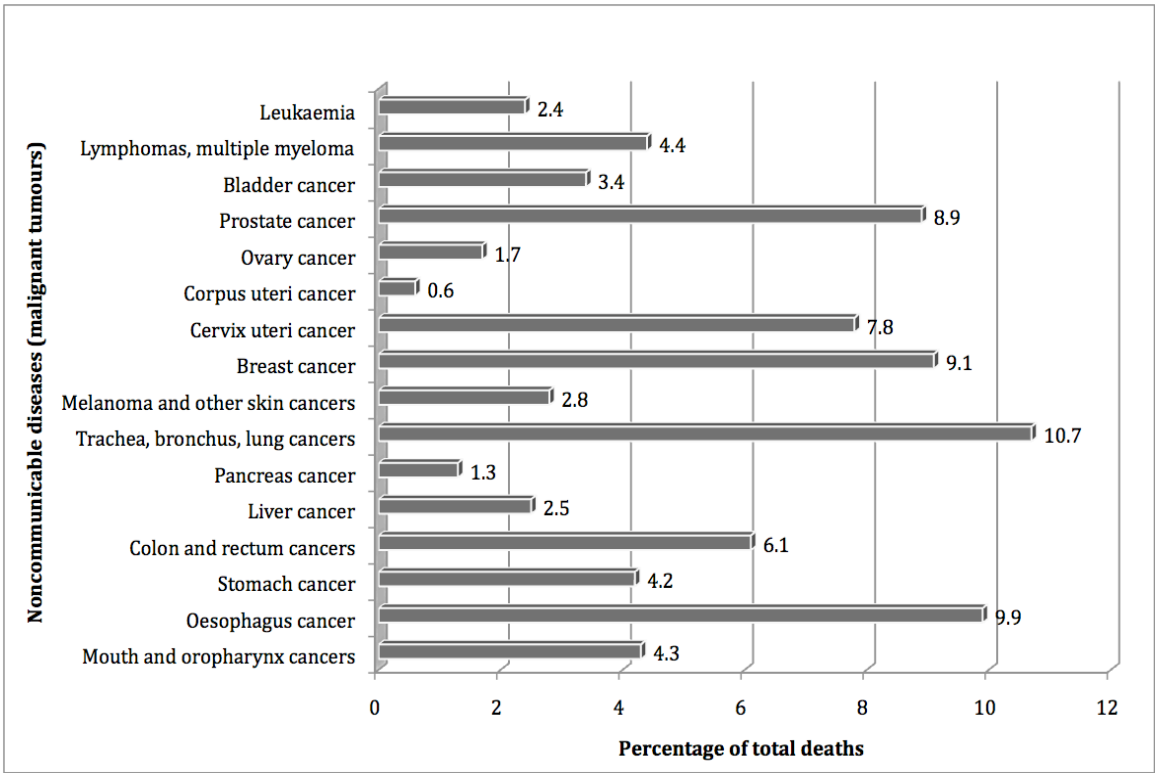


Figure 1: Estimated deaths per 100 000 population by cause in 2004, South Africa[3].

1.2 Classification of cancer

Cancers are classified according to the type of cell that constitute the tumor, and hence the assumed origin of the tumor, histology and the extent of the disease (http://www.oncologychannel.com/staging.shtml#staging, Retrieved May 22, 2010). This classification would aid in determining appropriate treatment as well as provide a more accurate prognosis (http://www.oncologychannel.com/staging.shtml#staging. Retrieved May 22, 2010). The type of tissue in which the cancer first occurs could vary from adenocarcinoma (affecting glandular tissue) to blastoma (affecting embryonic tissue of organs), leukemia (affecting tissue that forms blood cells), lymphoma (lymphatic tissue), myeloma (originating from bone marrow), carcinoma (malignant tumors derived from epithelial cells) or even sarcoma (originating from connective or supportive tissue) (http://www.oncologychannel.com/staging.shtml#staging.

Retrieved May 22, 2010). The extent of the disease is classified by the TNM method, tumour size (T), degree of node involvement (N) and distant metastasis (M) (http://www.oncologychannel.com/staging.shtml#staging. Retrieved May 22, 2010). A tumor given a M0 would suggest that no evidence of distant metastases has been noted while M1 would mean that distant metastasis is present. This can then be taken a step further with a numerical system providing a more detailed description of the extent of the disease (Table 1).

Table 1:Table showing the stages of cancer with stage IV correlating to a poor prognosis

Stage 0	Cancer *in situ* (limited to surface cells)
Stage I	Cancer limited to the tissue of origin, evidence of tumor growth
Stage II	Limited local spread of cancerous cells
Stage III	Extensive local and regional spread
Stage IV	Distant metastasis

The key factors that distinguish malignant tumors from benign tumors include the ability to infiltrate surrounding tissue, the destructive nature of the cells as well as its highly metastatic potential.

1.3 Progression of cancer

Cancer is a disease whereby mutations result in uncontrolled cell growth by either unregulated cell proliferation or the lack of apoptosis. These cells then continue to grow and mutate with the aid of oncogenes (e.g. Ras) or tumor suppressor genes (e.g. p53 and Rb) that act by altering cell cycle checkpoint regulators and the DNA repair system[4].

It has been shown that changes in the general apoptotic process could have a significant effect on the progression of tumors, suggesting the inactivation of apoptosis at the time of tumor progression[4]. It is suspected that most cancer types are able to induce changes that allow for the evasion of apoptosis (Figure 2). Mutations in *p53* leads to uncontrolled cell proliferation[4]. Loss of pro-apoptotic (e.g. Bax genes) regulation occurs as a result of this mutation. Small interfering RNAs (siRNAs) directed against LRP/LR lead to the down-regulation of LRP/LR which in turn lead to the induction of apoptosis in Hep3B cancer cells[5]. This suggests that LRP/LR may

play a role in cancer cell survival and may be a potential target for the induction of apoptosis in cancerous cells.

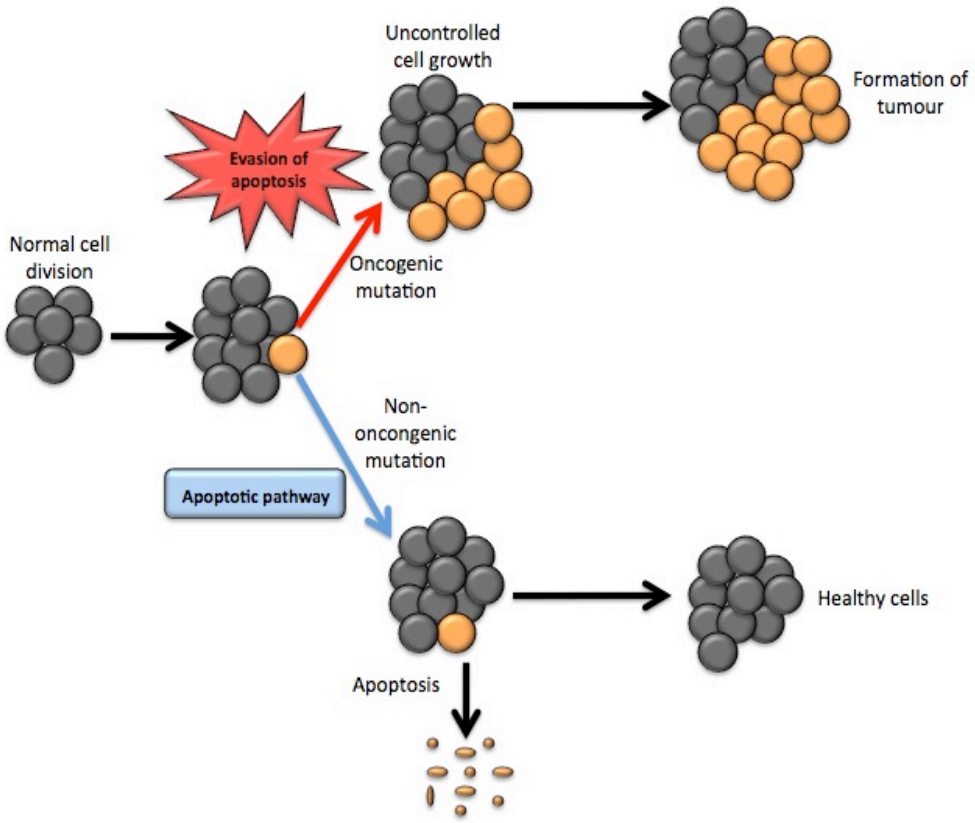


Figure 2: Comparison of normal and tumour cell division/proliferation. Healthy cells are displayed in grey and tumor cells in yellow. With the activation of oncogenes apoptosis is evaded and the tumor progresses. Non-oncogenic mutations induce apoptosis and allow for the continued proliferation of healthy cells[3].

1.4 Laminin

The Extracellular Matrix (ECM) provides structural support and is the defining feature of connective tissue. It comprises of an interstitial matrix but more importantly the basement membrane, which consists of the basal laminae and the reticular laminae. One of the primary components of the ECM is laminin, predominantly found in the basal laminae is known to form web-like networks and plays a critical role in cell adhesion as well in the binding of several other ECM components. Laminin was found to be involved in the assembly of the basement membrane[6], cell attachment[7], migration[8], growth[9], differentiation and angiogenesis[10]. Laminin has also been implicated in the induction of increased MMP2 activity. The interaction between laminin and cells by means of the 67kDa laminin receptor plays a critical role in

signal transduction pathways as well as possible involvement in kinase phosphatase cascades.

1.5 LRP/LR

The 37kDa / 67kDa laminin receptor precursor/high affinity laminin receptor (LRP/LR) is believed to play a significant role during cell invasion and therefore in the metastasis of various cancer types[3,11,12]. Several isoforms of the receptor have been found, with the most abundant being the 67kDa, which has a high affinity for laminin[3]. This receptor was first isolated from tumor cells[13] and offers two binding sites for laminin, a peptide G sequence (aa161-180) and another at the carboxy terminus (aa205-229). Furthermore, this protein acts as a receptor for the cellular prion protein (PrP^{c})[14], infectious prion protein (PrP^{Sc})[15], as well as some viruses such as Venezuelan equine encephalitis (VEE)[16], Dengue virus, Sindbis virus[17] and Adeno-associated virus (AAV) serotypes 8, 2, 3 and 9[18]. LRP/LR also provides binding sites for other extracellular components such as elastin and several carbohydrates[19]. Due to LRP/LR spanning the lipid bilayer as well as having the C-terminus situated in the extracellular space and a cytoplasmic N-terminus, it can be classified as a type II transmembrane protein (Figure 3).

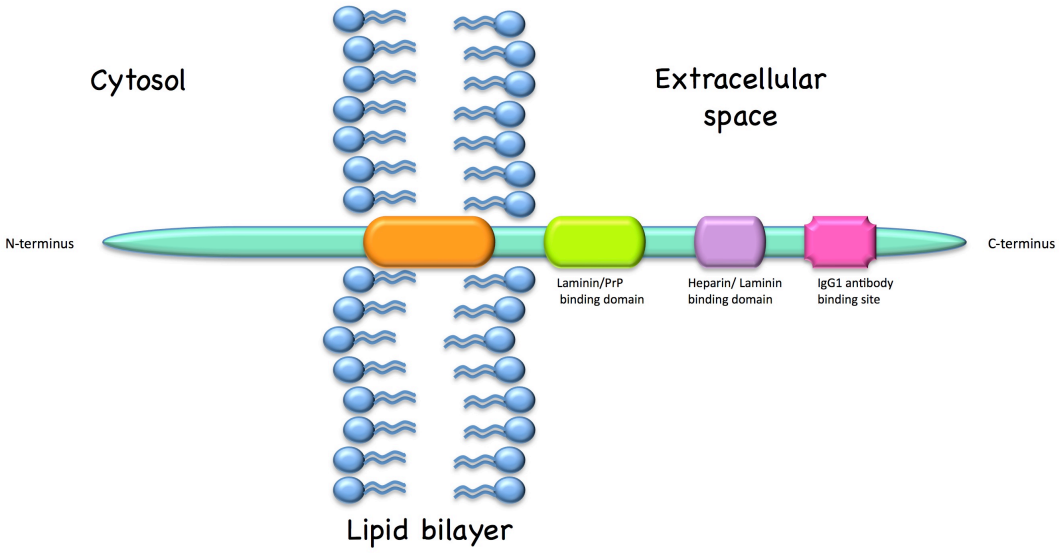


Figure 3: 37kDa laminin receptor precursor (LRP) on the cell surface showing the transmembrane domain in orange. It also shows the laminin/PrP binding domain in green, heparin/laminin binding domain in purple as well as the scFv/IgG1 antibody binding site indicated in pink, all of which form part of the receptor that is located in the extracellular space.

1.6 The 37kDa/67kDa LRP/LR and cancer

LRP/LR is a non-integrin laminin receptor that is involved in several tumorigenic processes, in particular, cell proliferation, cell viability, cell movement, cell adhesion and cell attachment[20]. The degree of metastasis of neoplastic cells is highly dependant on the interaction with LRP/LR, this in turn affects the general laminin mediated basement attachment and consequently, local cell degradation and movement[21]. Expression of the mature 67kDa form of the receptor is found on most normal cells, the immature 37kDa form has been noted as being an oncofetal antigen. A direct link between the over-expression of the 67kDa form and an increased invasiveness has been identified[5]. This trend was found particularly in gastric[22], colon[23], colorectal[24], cervical[25], breast[26], lung[13], ovarian[27], pancreatic[28] and prostate cancers[29]. This discovery has lead to the suggestion that the expression level of 67kDa laminin receptors could be a reliable method of prognosis for metastatic tumors[28,29]. Furthermore the over-expression of this receptor could provide an opportunity for cancer therapy directed at this site.

Human fibrosarcoma (HT-1080) cells that were pretreated with an anti-LRP antibody showed significantly reduced lung metastasis compared to untreated cells in a murine model[30]. *In vivo* studies demonstrated that suppression of LRP expression lead to a reduction in the proliferation and tumor formation of lung cancer cells[31]. Furthermore, the application of an anti-LRP/LR antibody (P4G) proved to have a significant regulatory effect and reduced lung metastasis in murine models[32].

Most forms of prion disease therapy directed at LRP/LR have the potential to be utilized in tumor intervening therapy. A study done using HT1080 cells have illustrated that the blocking or down-regulation of the LRP/LR receptor minimized the invasive potential of these cells[33]. Interference of the laminin-LRP interaction results in a significantly hindered invasion. Ways in which this can be achieved include anti-LRP/LR antibodies, such as full-length format (scFv) IgG1-iS18, as well as heparan mimetics and pentosan polysulfate[33]. The success of this brings forward the possibility of developing alternative methods capable of reducing the metastatic nature of cancer. Interestingly, a recent study has shown a definite link between LRP/LR and the maintenance of cell viability[5]. An increased level of LRP/LR found

on the neoplastic cell line HT-1080[33] in conjunction with the fact that LRP/LR inhibits apoptotic processes[5] indicates that the receptor plays a critical role in the progression of cancer and the development of metastatic tumors.

As mentioned previously, the LRP/LR plays a key role in tumorigenic processes including cell adhesion, angiogenesis[34] and cell migration[35]. Not only has the 67kDa high affinity laminin receptor found to be over-expressed in lung and breast carcinomas[36], auto-antibodies have been found in the blood of breast cancer patients directed against the 37kDa LRP[37]. A direct correlation between the 37kDa/67kDa LRP/LR level and the metastatic as well as invasive potential has also been observed[36].

The process of metastasis is complex and can be summarized as the following steps: breaking off from primary tumor, movement through blood vessels and finally the formation of a secondary tumor at a new location (Figure 4). Cell invasion is a critical event in the formation of metastasis and is mediated through attachment and degradation of Extracellular Matrix (ECM) components such as proteoglycans, collagens and laminins. This degradation is achieved with the use of various enzymes such as serine, threonine proteases and Matrix Metalloproteinases (MMP). The interaction between Laminin-1 and the 67kDa LR enhances the ability of tumorigenic cells to invade tissue due to the activation of these proteolytic enzymes[38]. These extracellular proteases, such as type IV-collagenase, which is an MMP, are able to degrade Laminin-1 as well as collagen type IV and lead to promotion of primary tumor cell migration through the ECM[39](Figure 5 & 6). Once the tumorigenic cell has traversed the basement membrane it is able to enter nearby vessels such as blood vessels and lymph. Once inside the vessel these cells may not survive due to the changes in the environment, as some are only able to remain viable if attached. Some tumorigenic cells may be recognized and neutralized by cells of the immune system, such as natural killer cells and natural killer T cells, which are the body's innate defense against metastasis. How and where the migrating cells stop is different for the various cancer types and once the tumorigenic cells are no longer moving, they can begin the process of forming a new tumor by leaving the blood vessel[40]. It then proliferates and a secondary tumor is formed due to the metastasis of the primary tumor cells.

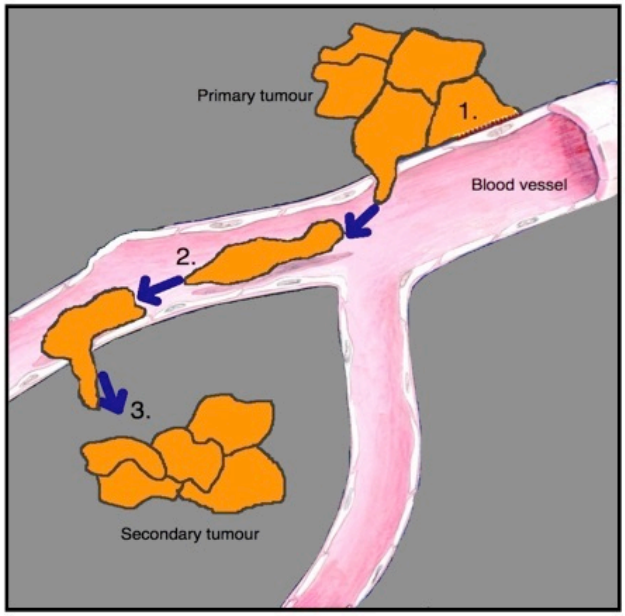


Figure 4: Illustration of the process of tumor metastasis. 1. Cells from original tumor attach to basement membrane of blood vessel and interact with the Laminin Receptor (LR). The basal lamina is then digested by MMP2/9 allowing for tumor cell entry into blood stream and 2. Migration. 3. A metastatic (secondary) tumor is then established by attachment of migrating cells to the blood vessel and movement into distal tissue[41].

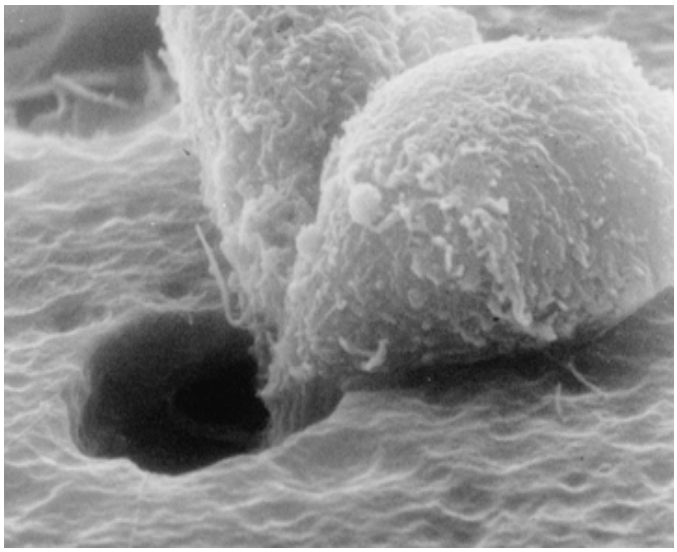


Figure 5: Electron micrograph showing HT1080 cells having digested Matrigel™ matrix migrating through 8µm pore of the membrane. (http://www.ebiotrade.com/buyf/productsf/BD%20Biocoat/354481.htm, Retrieved January 6, 2012).

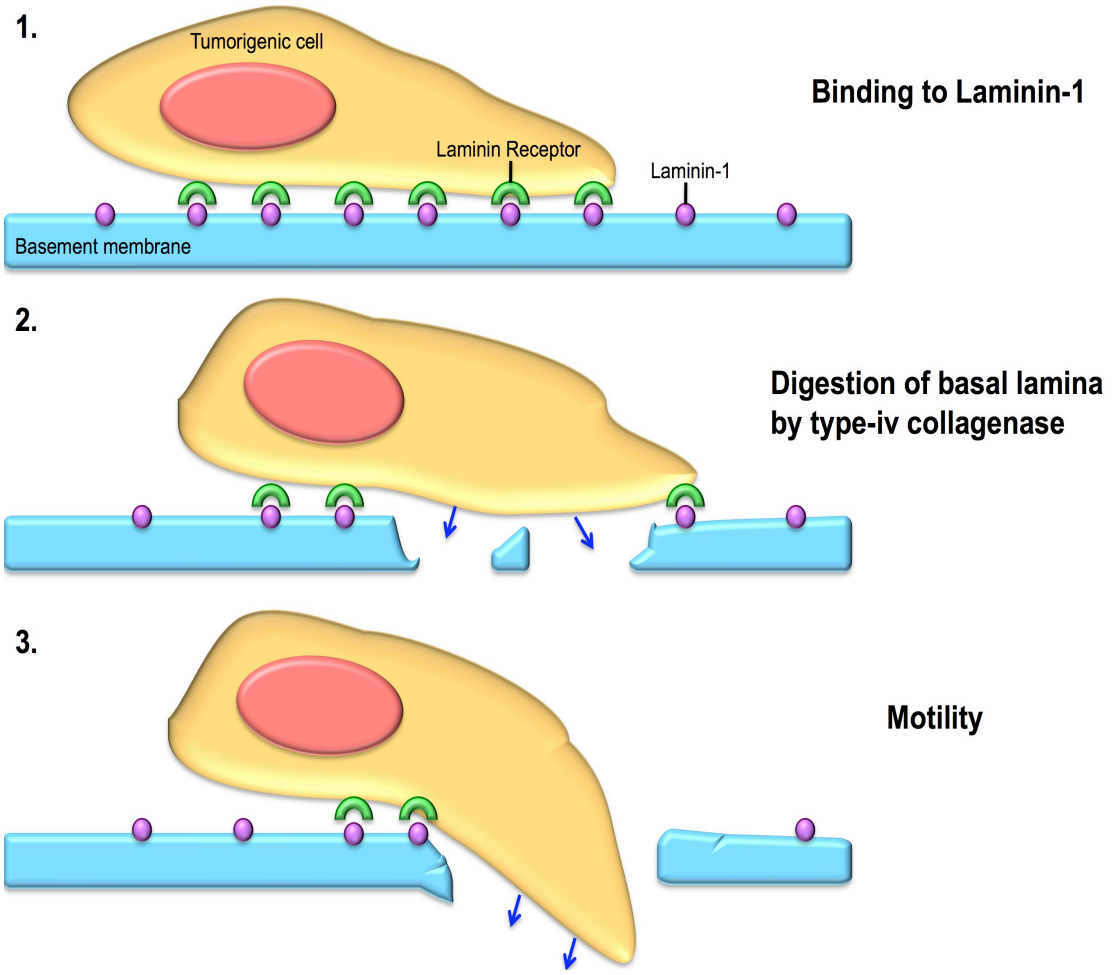


Figure 6: Schematic diagram illustrating cell invasion involving LRP/LR by cell adhesion, and MMP2/9 ECM degradation allowing for cell migration. 1.) Attachment of tumorigenic cell to Laminin-1 on the basement membrane via the Laminin Receptor, 2.) Digestion of the basal lamina by type IV collagenase secretion induced upon attachment, 3.) Degradation of the basement membrane allows for tumorigenic cell motility into the blood stream.

1.7 Antibodies

In order to neutralize antigens invading the body, immunoglobulins (Igs) also known as antibodies are synthesized. In most cases antigens are proteins, polysaccharides or nucleic acids originating from bacteria, viruses or other microorganisms. Immunoglobulins are full-length antibodies consisting of a heavy chain (HC) and a light (LC) chain (Figure 7). The former is built up of an antigen-binding variable domain and a constant domain. The latter, contains an N-terminal variable domain as well as a C-terminal domain that is constant. The variable domains are interchangeable between antibodies allowing for the binding of many different antigens.

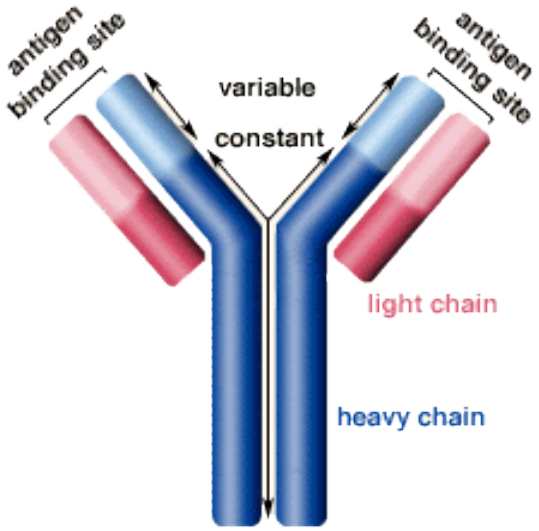


Figure 7: Illustration of a full-length immunoglobulin with its structural domains, showing the antigen binding sites as well as indicating (in red) the light chain and the heavy chain (in blue).

Currently, there are several ways of producing antibodies, however, very few are capable of producing monoclonal antibodies (MAb's) rather than polyclonal ones. Injecting rabbits with the appropriate antigen easily produces polyclonal antibodies. The serum from the rabbits' blood will then contain the antibodies against this antigen, as well as a host of other antibodies. The challenge at this stage is then isolating the required antibodies from this heterogenic solution, since in most cases it would prove to be ineffective as a therapeutic treatment. A polyclonal serum only

consists of 5-10% of the antibody directed against the antigen used for immunization[42]. Another disadvantage is that the amount of a polyclonal antibody that can be produced is limited. It is for these reasons that a technique was developed to produce a single class of antibodies in a serum (i.e. MAb's). The hybridoma technique involves the fusion of a short-living antibody producing cell with an immortal myeloma cell, resulting in the production of a single type of antibody[43]. This technique has opened up several windows of opportunity in the production of therapeutic antibodies. The development of monoclonal antibodies has offered new perspectives in therapeutic treatments. The over-expression of monoclonal antibodies in *Escherichia coli* has been successfully demonstrated[44].

1.8 Therapeutic antibodies

Monoclonal antibodies can be utilized as a therapeutic agent for the treatment of various diseases including cancer (Table 2). This is possible due to their ability to specifically bind to target cells or proteins and flag them for the destruction by the immune system (e.g. Herceptin)[45]. The mode of action of these antibodies can vary, and includes blocking specific receptors linked to tumor growth thereby hindering proliferation and progression. In other instances, such as in radio-immunotherapy a radioactive dose is localized on targeted cancer cells[46]. Antibody-drug conjugates (ADC's) are a revolutionary new form of therapeutic antibodies that are designed to combine monoclonal antibodies and their anti-cancer activities with potent cytotoxics[47]. These antibodies are able to selectively neutralize cancer cells while minimizing effects on normal tissue.

MAb's present a promising tool in metastatic cancer treatment and have been found to illicit appropriate immune responses in murine models[30]. The efficacy of these MAb's is highly dependant on their structures and consequently their half-lives, which can range from approximately 12 hours for single chain antibodies to 2-3 weeks for full-length antibodies[42]. A longer half-life is imperative for *in vivo* studies therefore, making full-length antibodies more suitable. Mammalian and bacterial cells differ as expression systems in terms of their expression level, growth speed and post-translational modifications. The expression of functional full-length immunoglobulins is not possible in *E. coli* since the bacterial translation machinery cannot perform

glycosylation and form sulfide bridges. It is for this reason that mammalian cells are used since protein synthesis in these cells results in the formation of the disulfide bonds, and correct folding within the Endoplasmatic Reticulum (ER). However, the antibodies must be secreted into the extracellular space to avoid exposure to the reducing environment inside the cells and this then warrants the formation of the disulfide bridges. The production of effective IgG's is made possible by co-transfecting the mammalian cells (HEK 293 EBNA) with plasmids encoding for the heavy and light chain.

Table 2: Currently available monoclonal antibodies for the treatment of cancer[46]

Antibody	Trade name	Approval date	Type	Target	Indication
Bevacizumab	Avastin	2004	Humanized	Vascular Endothelial Growth Factor (VEGF)	Colorectal cancer, lung cancer
Cetuximab	Erbitux	2004	Chimeric	Epidermal growth factor receptor	Colorectal cancer, head and neck cancer
Ipilimumab (MDX-101)	Yervoy	2011	Human	Blocks CTLA-4	Melanoma
Panitumumab	Vectibix	2006	Human	Epidermal growth factor receptor	Colorectal cancer
Trastuzumab	Herceptin	1998	Humanized	ErbB2	Breast cancer
Edrecolomab	Panorex	1995	Murine	EpCAM	Colorectal cancer

1.9 Anti-LRP/LR specific antibody IgG1-iS18

Since it has been found to be involved in several cancer-associated processes, LRP/LR would then serve as an obvious target in the treatment of metastatic cancer[32]. Studies have also shown the effective treatment of Prion diseases with the application of therapeutic antibodies that target LRP/LR[42,48,49]. The efficacy of this approach could be assessed by blocking the invasion of tumorigenic human fibrosarcoma HT-1080 cells by several anti-LRP/LR antibodies as well as anti-LRP/LR tools including siRNA and heparan mimetics[33]. siRNA's are small interfering RNA's and form a class of double-stranded RNA molecules that interfere with the expression of specific genes, while heparan mimetics act as competitors of endogenous heparan sulphates known to act as co-receptors in the process of metastasis. Anti-LRP/LR tools that have successfully impeded the invasive nature of HT1080 cells include the single-chain scFv iS18, the full-length IgG1-iS18 antibodies, the polysulfated glycans HM2602 and pentosan polysulfate (SP-54)[33]. It was found that the epitope for IgG1-iS18 antibody stretches from amino acid (aa) 272-280 of LRP: TEDWSAAPT[33]. This site is located close to the C-terminus end, which is exposed to the extracellular space, however it is not located in the direct laminin-binding site[50]. An indirect binding created by heparan sulfate proteoglycans is thought to be located in the 180-285aa region of LRP.

1. 10 Aims and objectives

Aim:

The aim of this study was to prove that the LRP/LR specific antibody (IgG1-iS18) significantly reduces the metastatic potential of important cancer types in South Africa.

Main objectives:

1. Determination of the surface level of LRP/LR by Fluorescent Activated Cell Scanning (FACS) on the following neoplastic cell lines HT-1080 (human fibrosarcoma cells), A-549 (human lung carcinoma cells), HeLa (human cervix carcinoma cells), MCF-7 (human breast carcinoma cells), SW-480 (human colon adenocarcinoma) and LNCaP (human prostate carcinoma).
2. Investigation of the invasive potential of the tumorigenic cells lines mentioned in 1 by performing invasion assays.
3. Investigation of a significant inhibitory effect of the anti-LRP/LR specific antibody IgG1-iS18 (IgG1-HD37 anti-CD19 for control) on invasion and adhesion of the tumorigenic cell lines mentioned in 1.

CHAPTER TWO – MATERIALS

2.1. Molecular biology

2.1.1 Plasmids

The following vectors encoding for the heavy and light chains of the full-length IgG1-iS18 anti-LRP/LR antibody and the full length IgG1-HD37 anti-CD19 were used:

- IgG1-iS18
  - pEU1.2VH_S18 (heavy chain)
  - pEU4.2VL_S18 5-4-1 (light chain)

- IgG1-HD37
  - pEU1.2VH/Fcg1 (heavy chain)
  - pEU1.2VL/Ckappa (light chain)

These plasmids were used to co-transfect HEK 293 EBNA cells to produce full-length antibodies.

2.1.2 Bacterial strains

Table 3: *E. coli* strain XL1Blu was used for the over-expression of the IgG encoding vectors

Media composition	
Luria Bertani (LB) medium	1% (w/v) Bacto-Trypton; 0.5% (w/v) Bacto-Yeast; 0.5% (w/v) NaCl
Luria Bertani (LB) Ampicillin medium	100μg/ml Ampicillin in LB medium

2.2 Cell culture

2.2.1 Eukaryotic cell lines

Table 4: Cell lines for *in vitro* experiments

Cell line	Cell type
Neoplastic	
HT-1080	Human fibrosarcoma (positive control)
A549	Human lung carcinoma
HeLa	Human cervix carcinoma
SW480	Human colon adenocarcinoma
LNCaP	Human prostate carcinoma
Negative control	
MCF-7	Human breast adenocarcinoma
NIH/3T3	Control mouse embryonic fibroblasts
Antibody production	
HEK293 EBNA	Human embryonic kidney cells expressing Epstein Barr Virus nuclear antigen

2.2.2 Cell culture media

The main cell lines require different media prepared from the following components:

- Dulbecco´s modified Eagle Medium (DMEM high glucose) (1x), with GlutaMAX ™ l, 4.500mg/L D-Glucose (HT-1080, A549, HeLa and MCF-7, NIH/3T3).
- RPMI 1640 (SW480 and LNCaP)

All the above culture media was supplemented with:

- 10% fetal calf serum (FCS) heat inactivated.
- 1% Penicillin-Streptomycin.

Additional supplements for cell culture:

- Dulbecco´s Phosphate-Buffered Saline (D-PBS) (1x) liquid.
- Trypsin/EDTA (1x).

Table 5: Storage of main cell lines needs special freezing media made up of the following

Cell line	Composition of specific freezing media
HT-1080	70% medium, 20% FCS, 10% DMSO, 1-2 x 10^6 cells/ vial
A549	70% medium, 20% FCS, 10% DMSO, 1-2 x 10^6 cells/ vial
HeLa	70% medium, 20% FCS, 10% DMSO, 1-2 x 10^6 cells/ vial
SW480	70% medium, 20% FCS, 10% DMSO, 1-2 x 10^6 cells/ vial
LNCaP	70% medium, 20% FCS, 10% DMSO, 2 x 10^6 cells/ vial
MCF-7	70% medium, 20% FCS, 10% DMSO, 1-2 x 10^6 cells/ vial
NIH/3T3	70% medium, 20% FCS, 10% DMSO, 1-2 x 10^6 cells/ vial

2.2.3 Cell culture material

To culture the eukaryotic cells the following material was required:

- Tissue culture (TC) flasks 75 cm² and 150 cm²
- Serological pipettes sterile (5 ml, 10 ml, 25 ml)
- Centrifugation tubes (15 ml, 50 ml)
- TC-Plates 24 well, 96 well
- Transwell culture plate inserts, millipore Ø 8µm
- Tissue culture dishes (Ø 150 x 20 mm)
- Transwell culture plate inserts, millipore Ø 8µm
- CryoTube™Vials

2.2.4 Material for cell lysates

- Lysis buffer:
  - 10 mM Tris/HCl pH 7.5
  - 100 mM NaCl
  - 10 mM EDTA
  - 0.5% (v/v) Nonidet-P40
  - 0.05% (w/v) Deoxycholic acid (DOC)
  - Stored at 4-8°C

2.2.5 Material for transient transfection

- Cells: HEK293 EBNA

- Plasmids:
  - pEU1.2VH_S18 (heavy chain)
  - pEU4.2VL_S18 5-4-1 (light chain)
  - pEU1.2VH/Fcg1 (heavy chain)
  - pEU1.2VL/Ckappa (light chain)

- 2xHEBS buffer: 280 mM NaCl; 1.5 mM Na_2HPO_4; 50 mM HEPES; pH 7.05
- 250 mM $CaCl_2$
- Media:
  - DMEM high glucose, 10% FCS 1% P/S
  - DMEM high glucose, 1% P/S, 1% Insulin-Transferrin-Selenium

2.2.6 Material for invasion and adhesion assays

- Cells: HT-1080, HeLa, A549, MCF-7, SW480, LNCaP
- Antibodies: IgG1-iS18, IgG1-HD37
- Media: 1%, 10% FCS and serum-free variants of the corresponding cell media
- 96-well plate
- 1% SDS Solution
- 1x PBS Solution
- 0.5% Toluidine Blue
- 0.5% Trypan Blue
- Neubauer haemocytometer
- Matrigel™
- Media containing agar
- Laminin-1
- Blocking solution
- 0.1% Crystal Violet
- 3.7% Formaldehyde
- 33% Acetic acid

2.3 Protein biochemistry

2.3.1. Solutions and reagents

Table 6: Solutions used in SDS-PAGE

SDS-PAGE	
Ammonium peroxisulphate (APS)	10% in ddH_2O
Upper Tris Buffer	0.5 M Tris, pH 6.8 4g/L SDS
Lower Tris Buffer	3 M Tris, pH 8.8 4g/L SDS
10x SDS running buffer	250 mM Tris, 1.92 mM Glycine in ddH_2O and 10% SDS
1x SDS running buffer	1% 10x SDS running buffer
5x SDS loading buffer	30% Glycerine, 312 mM Tris/HCl pH 6.8, 10% SDS
Coomassie staining	1.5 g/l Coomassie Brilliant Blue R250, 10% acetic acid, 30% ethanol in ddH_2O
Destaining solution	10% acetic acid, 30% ethanol in ddH_2O

Table 7: Solutions used in Western Blotting

Western Blotting	
10x PBS	80 g NaCl, 2.0 g KCl, 14.4 g Na_2HPO_4 x $2H_2O$, 2.4 g KH_2PO_4, ddH_2O pH 7.4
1x PBS Tween	1% 10x PBS, 0.1% TWEEN 20 in ddH_2O
1x Transfer Buffer	20% methanol in 25 mM Tris and 19.2 mM Glycine
Blocking Buffer	3% Non-fat milk in 1x PBS-Tween
Washing Buffer	1x PBS-Tween
Stripping solution	1% SDS, 1mM Glycine, 0.1% Nonidet-P40, pH 2.2

Table 8: Solutions used in IgG purification

IgG purification	
Steritop filter blocking solution	150 ml 2% BSA in ddH_2O
Wash/Binding buffer	DMEM high glucose with GlutaMAX™ l, 4.500 mg/L D-Glucose, pH 7
Elution buffer	0.1M Glycine HCl pH2.7, 140mM NaCl
IgG storage buffer	1M Tris/HCl pH 8.8
Column storage solution	20% ethanol
Dialysis buffer	1x PBS

2.3.2. Antibodies

Table 9: Different antibodies were used in the various analyses

Western Blotting	
Detection of LRP/LR	
Primary Antibody	IgG1-iS18 (1:10000)
Secondary Antibody	Goat-anti-human-POD (1:5000)
Tertiary Antibody	Anti-rabbit
Detection of ß-Actin	
Primary Antibody	Mouse-anti- ß-Actin (1:5000)
Secondary Antibody	Rabbit-anti-mouse IgG1-POD (1:5000)
Fluorescence activated cell scanning (FACS)	
Detection of LRP/LR	
Primary Antibody	IgG1-iS18 (1:100)
Secondary Antibody	Rabbit polyclonal to human IgG-H&L (FITC coupled)(1:100)

Note: All dilutions were done in 10% horse serum in 1x PBS-T or 5% milk powder in 0.2% 1xPBS-T(1% 10x PBS, 0.2% TWEEN 20 in ddH_2O)

CHAPTER THREE – METHODS

3.1. Molecular biology

3.1.1 Plasmid DNA isolation

Plasmid isolation was done using a Plasmid Mega and Maxi Prep Kit according to the manufacturers protocol (Qiagen, Invitrogen). It is based on the alkaline lysis procedure whereby chromosomal and plasmid DNA are denatured, however selected plasmid DNA is re-natured under neutralization. This was then purified by anion exchange chromatography and isopropanol precipitation. After washing with 70% ethanol it was then air-dried and dissolved in TE-buffer. Plasmid DNA was quantified by NanoDrop® ND-1000. This is a full-spectrum (220-750nm) spectrophotometer that was used to measure small samples (~2µl) with high accuracy. It is able to analyze sample absorption and determine the concentration.

3.2. Cell culture

3.2.1 Cell cultivation

The various cell lines were cultivated in the appropriate medium at 37°C in a humidified 5% CO_2 atmosphere (Incubator from Heraeus), using tissue culture dishes (Ø 150 x 20 mm). Following the removal of media, confluent cells were washed with 5 ml PBS and detached with 1 ml of Trypsin/EDTA. Cell detachment was stopped by addition of 8.5 ml of media containing 10% FCS and detached cells were passaged in dilutions ranging from 1:2 to 1:25 in order to maintain optimal growth.

3.2.2 Freezing and thawing of cells

Freezing of cells:

The various cell lines were frozen for safekeeping. Confluent cells were detached and centrifuged at 1200rpm for 10 minutes. The resulting pellet was then re-suspended in freezing media. Aliquots (1ml) of the suspension were then frozen for 24 hours at -20°C and finally stored at -80°C until needed.

Thawing of cells:

Frozen cells were removed from a -80°C freezer and thawed on ice. Thawed cells were transferred to the appropriate media containing 1% Penicillin/Streptomycin and

20% FCS. This was then centrifuged at 1200rpm for 5 minutes and the pellet re-suspended in the same media used previously. Cell suspension was transferred to a cell culture dish and incubated at 37°C, 5% CO_2. The growth of the cells was monitored over the next 5 hours and the media changed to 10% FCS upon cell attachment.

3.2.3 Cell count determination

In order to maintain a constant number of cells during experiments with the various cell lines, a cell count was performed. This involves Trypan-blue staining where viable cells appear clear and dead cells stain blue. These cells can then be counted using a Neubauer haemocytometer. Briefly, cells were washed with DPBS, detached with Trypsin/EDTA and suspended in the appropriate media. An aliquot of the cell suspension was mixed with the equivalent amount of Trypan-blue solution (0.4 %). 10 µl was placed on the haemocytometer and the mean cell average in 16 small squares counted under the light microscope. The cell number was then calculated according to following formula:

$$\text{Mean average of cells in } \frac{\text{16 small squares x } 10^4}{4} = \text{number of cells/ml.}$$

3.2.4 Preparation of cell lysates

Cells were washed with DPBS and detached in the same manner mentioned previously. The suspension was then centrifuged for 10 minutes at 1200rpm and the pellet re-suspended in 500 µl of lysis buffer. Following 15 minutes incubation on ice, lysates were centrifuged at 14000 rpm for 2 minutes.

3.2.5 BCA™ protein assay

The BCA™ Protein Assay is a method used to quantify the total level of protein in a solution by colorimetric analysis. It is based on the reduction of Cu^{2+} to Cu^{+} by the peptide bonds found in proteins, and the formation of a violet complex of Cu^{+} with bicinchoninic acid (BCA, 2,2´-Bichinolin-4,4´-dicarbonicacid). The amount of Cu^{2+} that is reduced is an indication of the protein concentration present in the sample. Following an incubation at room temperature, the absorbance was measured at 562nm using an ELISA reader.

3.3 Antibody production

3.3.1 Synthesis of IgG1-iS18 and IgG1-HD37 in mammalian cells

Human embryonic kidney 293 (HEK 293 EBNA) cells stably transfected with the Epstein-Barr virus EBNA 1 gene were transiently transfected with the plasmids encoding for the IgG1 antibodies. The EBV EBNA 1 protein has been shown to give a significantly higher expression level if a vector (such as the IgG1-iS18 encoding vector) contains oriP of EBV and would therefore result in a high yield expression.
Calcium phosphate precipitation was used for the transfection of the mammalian cells. Calcium phosphate is precipitated from a HEPES-buffered saline solution (2xHEPES) containing phosphate ions and a Calcium chloride solution. The DNA to be transfected then binds to this precipitate and thereafter is taken up by the target cells via endocytosis. After it is released into the cytoplasm of the cell, the DNA is transported into the nucleus to be transcribed. Cultured HEK 293 EBNA cells were transfected with the plasmid encoding for the heavy and light chains. Following an incubation time of 16 hours with the plasmid, the mammalian cells were washed with DPBS and re-suspended in pre-warmed media containing ITS (Insulin-Transferrin-Selenium). After 24 hours the supernatant containing the secreted antibodies was collected and the cells re-suspended in ITS supplemented media for a further 24 hours. The supernatant was then centrifuged for 10 minutes at 1200rpm to remove debris and stored at -80°C until it was purified.

3.3.2 Purification of IgG1-iS18 and –HD37 by protein A sepharose affinity chromatography

Affinity chromatography was employed as the method of purifying the solution containing the antibodies that were produced by the HEK 293 EBNA cells. The process is based on the principle of antigen-antibody binding between an immobilization phase and the proteins of interest. Protein A Sepharose™ contains receptor molecules derived from the bacteria *Staphylococcus aureus*. These molecules provide four high affinity (K_A 10^6/M) binding sites that are able to bind to the F_c regions of immunoglobulins (IgG) of many mammalian species through heavy chain interactions.

The purification involves multi-step chromatography and immobilized by generating a stable thioether linkage to Sepharose 4 Fast Flow. This highly cross linked, 4% agarose derivate base matrix and the high affinity binding of Protein A allow for rapid processing of large volumes of dilute cell culture fluid, and was therefore the most appropriate method for the purification of the antibodies.

3.3.3 Dialysis of IgG1-iS18 and IgG1-HD37

Dialysis is a term frequently mentioned in the literature as a technique to remove salt or other small molecules and to exchange buffer composition of a sample. Since the molecular weight of IgG is 150kDa and the molecular weight of the unwanted salts are 100-5000Da, the membrane used in the dialysis had a Molecular Weight Cut Off (MWCO) of 2000-5000Da. The cellulose membrane consists of cross-linked cellulose fibres making the pores irregular gaps of varying form and size instead of defined holes. Since the permeability of the membrane also depends on other factors such as the molecular shape, globular molecules are retained more efficiently than fibrillar molecules. Therefore, dialysis cannot perform strict separation of molecules, but simply an accumulation of big molecules inside the tube and sufficient removal of unwanted molecules such as salts. This is done in a beaker filled with dialysis buffer (1% PBS) on a magnetic stirrer at 4°C for 18 hours. The dialysis buffer was changed twice during this period. Following dialysis the membranes were rinsed with sterile distilled water and the antibody stored at -20°C. All materials during this procedure were sterilized and the resulting preparation was handled aseptically.

3.3.4 Detection of IgG1-iS18 and IgG1-HD37

Detection of the antibody produced was done using SDS-PAGE and subsequent overnight staining of the gel with Coomassie Blue. De-staining was then performed by cooking the gel in water for 3 x 5 minute periods in the microwave. Gel-doc imaging was used to record the bands present.

3.3.5 Quantification of IgG1-iS18 and IgG1-HD37

The antibody present in the solution consequent to the dialysis was quantified using a Nano-drop (280nm) with the storage buffer serving as the blank.

3.4 FACS (Fluorescence activated cell scanning)

Fluorescence activated cell sorting/scanning is a method employed to determine the expression level of proteins or to separate cells according to their surface protein expression. This method was used to determine the cell surface levels of LRP/LR on tumorigenic cell lines. The protein of interest was detected with an antibody, and a fluorescence dye (e.g. FITC) labeled secondary antibody directed against the primary antibody. A blue argon laser in a flow cytometer distinguished the labeled from the unlabeled cells from the fluorescence emitted by the FITC. FITC has excitation and emission spectrum peak wavelengths of approximately 495nm/521nm and the fluorescence detected by the FL1 channel. Samples were tested with both the IgG1-iS18 and IgG1-HD37 antibodies and with the FITC labeled antibody only in order to detect possible background emission. Confluent cells were detached and centrifuged for 10 min at 1200 rpm, with the resultant pellet re-suspended in 1 ml 4% PFA and incubated for 10 minutes at 4°C in order to fix them. This step was then followed by another centrifugation of 10 min at 4000 rpm, and the pellet re-suspended in 1ml FACS-buffer. At this point the cell suspension was then separated into 2 even halves and centrifuged in the same manner. One of the pellets was re-suspended in 100 ml of the primary anti-LRP/LR antibody IgG1-iS18 (c=30mg/ml), while to the other one with 100 ml of FACS-buffer only (incubation time of 2 hours). After 3 washing steps, 100 µl of secondary anti-human-FITC antibody (c=20mg/ml) was added to both samples and once again incubated for 2 hours. The samples containing the secondary antibody only, acted as a control for background emission. After washing the samples another 3 times, the cells were finally re-suspended in 1ml of FACS-buffer and 10 000 cells measured by FACS (Beckmann COULTER EPICS® XL-MCL).

3.5 Invasion assays

The experimental approach to determine the potential of cells to invade an extracellular matrix (ECM) is the chemo-invasion assay. It makes use of a chemo-attractant on the lower site of a polycarbonate filter to introduce cell invasion through an ECM-like Matrigel™ and the pores of a filter membrane by chemotaxis (Figure 8). The pore size has to be big enough for the cells to move through but must be small enough for them not to fall through. For eukaryotic cells the optimal pore size is at approximately 8µm. The attractant can vary but in this case 10% FCS was used. The period of incubation time is a major factor for the success of the assay, since incubation for too long would lead to migration into the reservoir and would distort the result, while a short incubation would lead to insignificant results. Due to this and the different invasive potentials, incubation time has to be adjusted and optimized. The Matrigel™, which was used, mimicked the basement membrane with its major components being laminin, collagen IV, and heparan sulfate proteoglycans.

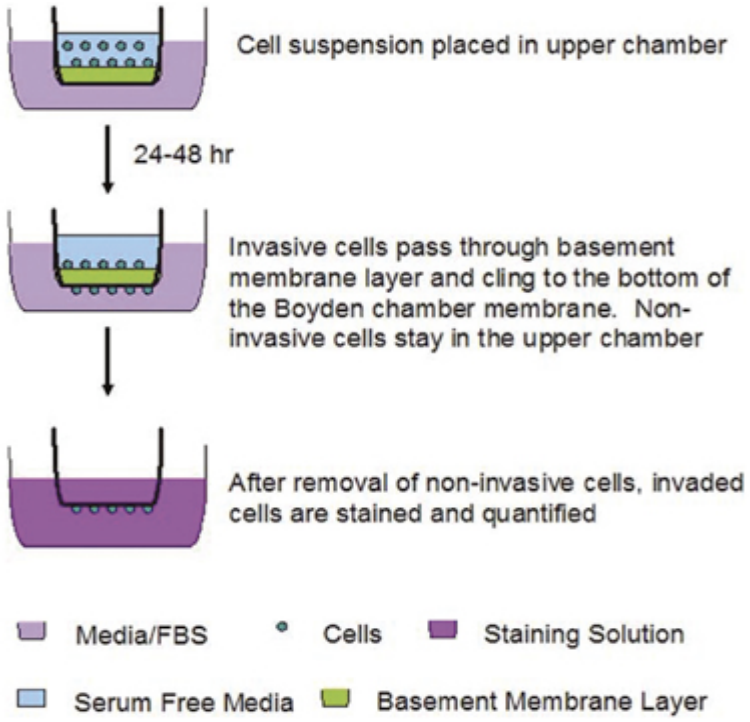


Figure 8: Principle of invasion assay – cells invading transwell insert with membrane (8µm pore size) and Matrigel™. This system serves as a model to mimic the interaction with the basement membrane. Cells with invasive potential are able to move through the pores and the Matrigel™ as they are drawn toward the chemo-attractant (10% FCS). Note, in the diagram FBS represents FCS.
(http://www.cellbiolabs.com/sites/default/files/CBA-110%20Fig%201.jpg)

3.5.1 Preparation of Transwell inserts, cells and determination of invasive potential

Matrigel™ was diluted to 1mg/ml in serum-free cell culture media. 100µl of the diluted Matrigel™ was transferred to the upper chamber of a 24-well transwell plate. This was then incubated at 37°C for 6 hours, during which time it formed a gel. The harvested cells were then washed with culture media (1% FCS) and re-suspended in this same media at a concentration of $1x10^6$ cells/ml. It is at this point that cells are incubated with the IgG1-iS18 antibody or the control IgG1-HD37 antibody for 10 minutes. 100µl of the cell suspension was loaded on to the gel while the lower chamber was filled with 500µl of serum-free culture media for the control and 500µl of culture media containing 10% FCS for the rest. This was then incubated at 37°C for 18hours. Samples were taken at certain time intervals in order to ascertain the ideal incubation time. Thereafter the upper and lower media were removed and the cells fixed with 300µl of 4% Paraformaldehyde (PFA), rinsed with 300µl DPBS and subsequently stained with 100µl of 0.5% Toluidine blue. Non-invading cells were then scraped off with a cotton swab and the dye on the invasive cells extracted with 300µl 1% SDS. The resulting solutions were then transferred to a 96 well microtiter plate and the absorbance was determined at 620nm in an ELISA reader. Experiments were performed in triplicate. As mentioned, cells placed in reservoirs containing serum-free media acted as negative controls in conjunction with cells incubated with the IgG1-HD37 control antibody.

3.6 Adhesion assay

To determine the ability of certain cell lines to adhere to a specific adhesive substrate, the adhesion assay was performed in 96-well plates coated with Laminin-1. To evaluate the efficacy of the anti-LRP/LR antibody, the cells were pre-incubated for 10 minutes with IgG1-iS18 and IgG1-HD37 (as a negative control). The surface of a 96-well plate was incubated with blocking solution (1% FCS in PBS). Cells suspended in serum-free media were added to the wells and incubated for 1 hour. After 1-hour incubation the attached cells were thoroughly washed with PBS, fixed in 3.7% PFA and then stained with 0.1% crystal violet. The pigment was extracted with 1% SDS and the absorbance was measured at 570 nm. This absorbance acted as an indicator of cells attached to Laminin-1 (Figure 9).

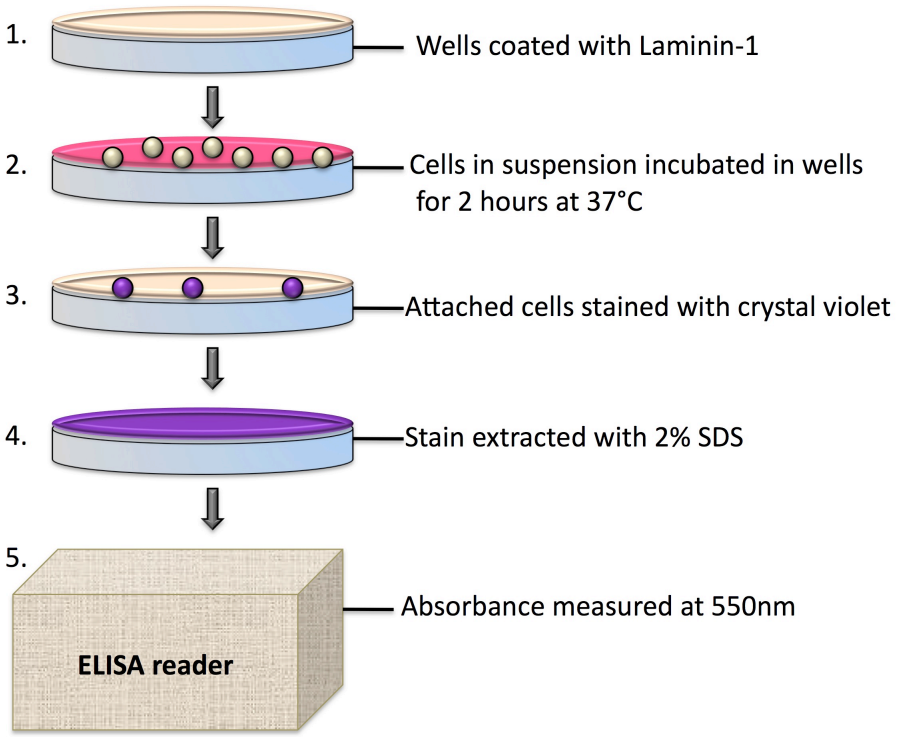


Figure 9: Illustration of the adhesion assay where wells are coated with Laminin-1 and cells are then incubated in these wells, attached cells are then stained and this absorbance measured. The amount of dye extracted being a representation of the number of cells that had attached.

3.7 Protein Biochemistry

3.7.1 Sodium dodecyl sulfate polyacrylamide gel electrophoresis (SDS-PAGE)

In order to visualize the relative protein expression and total LRP/LR levels in tumorigenic cell lines an SDS-PAGE was performed. This technique is able to separate proteins according to their electrophoretic mobility. These proteins are heat denatured in the presence of the detergent sodium dodecyl sulfate (SDS) and the reducing agents dithiothreitol (DTT) or ß-mercaptoethanol. The manner in which SDS denatures the proteins is by firstly disrupting non-covalent bonds resulting in the loss of their native conformation. A negative charge then forms on the protein due to the binding of anions. However, due to the proteins native charge an electrostatic repulsion occurs resulting in the unfolding of the protein. Following the addition of SDS proteins become negatively charged overall. In the consequent separation by electrophoresis, a polyacrylamide gel acts as a sieve in which smaller proteins are able to travel further. Therefore, the mobility (linear function of the logarithm) of a protein shall serve as an indication of its molecular weight. The pore size of a gel can be altered by adjusting the amount of acrylamide, and cross-linkage with polymerization following the addition of APS (Ammonium persulfate) and TEMED (N, N, N', N'-tetramethylethylenediamine). In this study it was necessary to separate proteins in the range of 10-100kDa in size. For this, 12% polyacrylamide gels were used. Protein markers were loaded on each gel and served as a reference for protein sample sizes.

3.7.2 Western Blotting

Western Blotting is an analytical technique used to detect specific proteins. This is achieved by firstly separating the proteins using gel electrophoresis (e.g. SDS-PAGE) and the resultant proteins are then electro-transferred to a membrane (e.g. PVDF, Nitrocellulose). This membrane is then probed using antibodies that contain binding sites specific for the protein you wish to detect. Finally, the secondary peroxidase-coupled (POD) antibody, catalyses light emission from the oxidation of luminol at 428 nm and the light emission from the resulting reaction and is then captured on x-ray film.

Cell lysates were prepared following the method mentioned previously and the BCA™ protein assay (please refer to 3.2.5.) was then employed to quantify the total protein levels and standardized the amount of protein that was loaded on to the SDS-polyacrylamide gel. The protein transfer was performed electrophoretically on PVDF (Biotrace™ PVDF Blotting membrane, 0.45µm pore size, Pall Corporation) in a PerfectBlue™ Semi-Dry Electroblotter (Peqlab) chamber according to the manufacturer's instructions. The PVDF membrane was first equilibrated in methanol and then placed in transfer buffer, and filter paper which was soaked in transfer buffer prior to transfer. The blotting procedure was carried out at 350mA for 45 minutes (Figure 10).

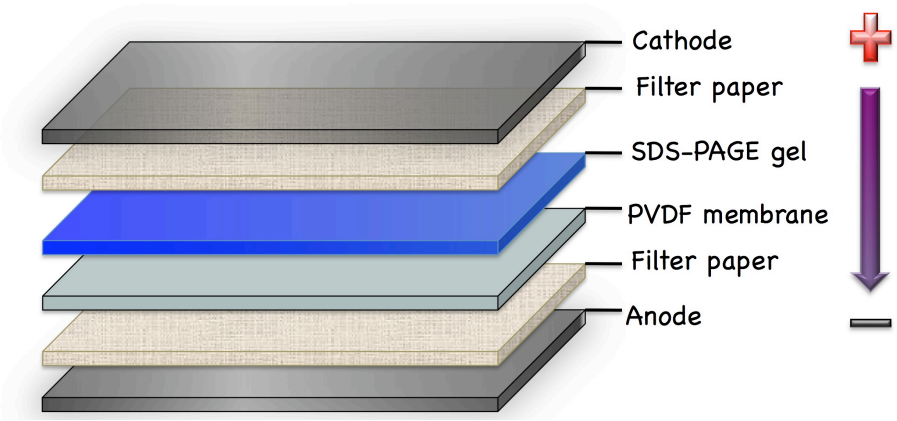


Figure 10: Principle of the semi-dry Transfer Western Blotting method

3.7.3 Protein detection and chemiluminescence

Due to the proteins being bound to the membrane, non-specific binding sites were blocked with blocking buffer for 1 hour. The membrane was then incubated in the primary antibody solution for 1 hour at room temperature. Subsequent to this, the membrane was washed then incubated with the appropriate secondary antibody for 1 hour at room temperature and detection done immediately after 3 x 10-minute washes. The secondary antibody used in the Western Blotting procedure is coupled with a peroxidase. Peroxidases, such as the horseradish peroxidase, catalyze the oxidation of luminol resulting in the emission of light (Figure 11). Antibodies labeled with horseradish peroxidase are able to react directly with immobilized protein antigens. For detection of the target proteins in this study SuperSignal WestPico Chemiluminescent Substrate was employed. Following the addition of 1ml of stable peroxide solution and 1ml of luminol/enhancer solution, fluorescence was visible and captured on x-ray film that was then developed.

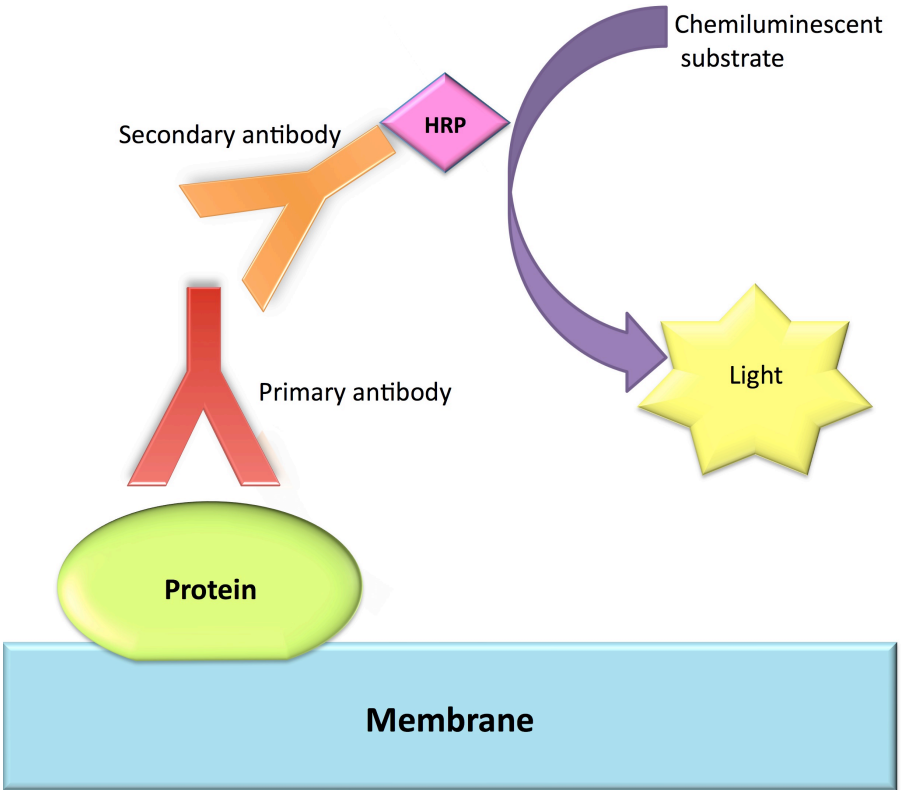


Figure 11: Immuno-detection of proteins showing the protein bound to the membrane, the primary antibody (1°Ab) attached to this, and the secondary antibody (2°Ab) attached to the 1°Ab. The figure also shows the Horse-Radish Peroxidase (HRP) and the oxidation of luminol resulting in light emission.

3.8 Data analysis and statistical evaluation

Statistical analyses were performed using a two-tailed Student's t-test with a 95% confidence interval. *p*-Values of less than 0.05 were considered significant.

* $p < 0.05$, ** $p < 0.01$, *** $p < 0.001$. The linear dependence between two variables was expressed using Pearson's (r) correlation coefficient.

CHAPTER FOUR – RESULTS

4.1 Production of anti-LRP/LR specific antibody IgG1-iS18 in mammalian cells

The synthesis of antibodies in most cases is achieved by employing two vector DNA molecules, one that carries the light-chain gene and the other that carries the heavy-chain gene. However, this approach could result in an imbalance of the biosynthesis of two polypeptides, i.e. the heavy and light chains. It is for this reason that careful consideration and calculation of the HC:LC is done in order to utilize the optimal ratio for IgG1 assembly in the ER[51].

4.1.1 Characterization of the plasmids

Plasmid DNA was prepared from pEU1.2VH_S18 encoding for the heavy chain of the antibody IgG1-iS18 and pEU4.2VL_S1 5-4-1 which encodes for the light chain of the anti-LRP/LR specific antibody IgG1-iS18[33]. pEU1.2VH/Fcγ1 encoding for the heavy chain of IgG1-HD37 and pEU1.2VL/Cκ encoding for the light chain of IgG1-HD37[33]. The IgG1-HD37 served as the control antibody directed against CD19 on the surface of human B cells. These vectors were amplified in *E. coli* and the DNA extracted and purified using the GenElute HP Plasmid maxi preparation kit (Sigma). Approximately 300-1000ng/μl of purified plasmid was obtained from a 300ml bacterial culture corresponding to each vector.

4.1.2 Antibody over-expression in HEK293 EBNA cells

The full-length anti-LRP/LR IgG1-iS18 and anti-CD19 IgG1-HD37 antibodies were successfully produced in HEK293 EBNA cells by co-transfecting the vector encoding for the heavy and the light chains in the ratio 53ng:36ng (HC:LC). HEK293 EBNA cells are human embryonic kidney 293 cells stably transformed with the EBV EBNA-1 gene. This cell line was chosen since the vectors encoding for the heavy and light chains have EBV oriP, resulting in an increased protein expression in the presence of EBNA-1[52]. Transfection was performed using the calcium phosphate precipitation method. Supernatants were collected over 24-hour and 48-hour periods, following transfection as described in the Materials and Methods section. 1 litre of culture medium was collected after each transient transfection and this was then purified.

4.1.3 Purification and detection of IgG1-iS18 and IgG1-HD37

1 litre of supernatant collected from transiently transfected HEK293 EBNA cells was filtered by Protein A Sepharose™ affinity chromatography. The protein A is able to bind immunoglobulin's through the interaction with the fc region of the heavy chain. The antibodies that had bound to the column were eluted using a low pH buffer and the collected fractions (2ml each) were then analyzed by 12% SDS-PAGE. The full-length antibody has a molecular weight of approximately 150kDa. Under reducing conditions, the disulphide bridges linking the heavy and light chains are disrupted and this will give rise to the appearance of 2 bands on the SDS-PAGE gel, at 50kDa (heavy chain) and 25kDa (light chain), respectively (Figure 12). Both IgG1-iS18 and IgG1-HD37 were successfully over-expressed in HEK293 EBNA cells. A total yield of 1μg/μl purified IgG1-iS18 and 1,5μg/μl purified IgG1-HD37 were obtained per 1l of culture medium, this was then utilized in subsequent experiments.

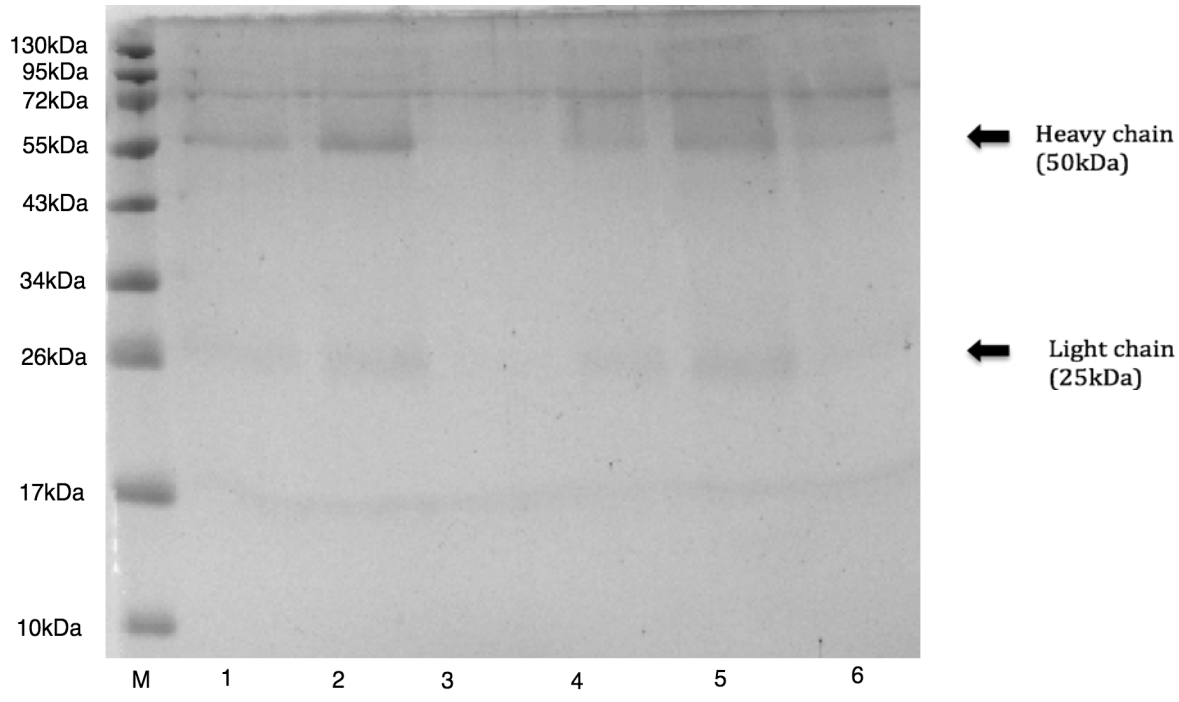


Figure 12: Biochemical analysis of IgG1-iS18 and IgG1-HD37 over-pressed in HEK293 EBNA cells co-transfected with vectors encoding for the heavy and light chains. SDS-PAGE and Coomassie blue staining of the IgG1-iS18 following Protein A Sepharose™ purification and dialysis (lanes 1, 2, 3), and IgG1-HD37 (lanes 4, 5, 6) purified from HEK293 EBNA cells after protein A sepharose purification and dialysis. The heavy chain can be seen at 50kDa and the light chain at around 25kDa.

4.1.4 Dialysis of IgG1-iS18 and IgG1-HD37

Dialysis is not only used to remove low molecular weight contaminants, such as salt, but also for buffer exchange prior to or after different chromatographic steps, in this case it was employed following Protein A Sepharose™ affinity chromatography. The molecular weight of IgG is 150kDa and that of the unwanted salts ranges between 2000 and 5000Da. A micro-dialysis unit with a cut off at 5000Da retained the antibody as the salts diffused out.

4.1.5 Characterization of IgG1-iS18

The purified antibody was then used in a Western Blot analysis to test its binding capability and specificity. It was found to successfully bind to the 37kDa LRP in several neoplastic cell lines, also, the secondary goat anti-human antibody was able to bind to the already bound IgG1-iS18 and upon application of the substrate fluorescence was visible (Figure 13).

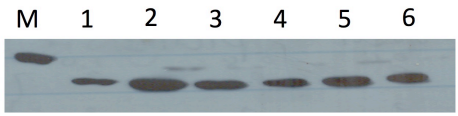


Figure 13: Western Blotting detection of 37kDa LRP from various neoplastic cell lysates by purified IgG1-iS18 antibody. In each lane, the same amount of total protein was loaded; lysates were separated by SDS-PAGE and transferred to a PVDF membrane. The marker is shown and in lane 1 SW480, lane 2 LNCaP, lane 3 HeLa, lane 4 A549, lane 5 HT-1080 and lane 6 NIH/3T3.

4.2 LRP levels

4.2.1 Cell surface LRP levels

Tumorigenic cell lines reveal a significantly increased cell surface LRP/LR level compared to the non-tumorigenic cell line NIH/3T3

A key factor in the process of metastasis is the interaction of the LRP/LR located on the surface of neoplastic cells, and Laminin-1. Therefore the cell surface levels of LRP/LR were investigated in order to ascertain if an increased LRP/LR level would result in an increased invasive potential. Cell surface levels of LRP/LR on the various neoplastic cell lines, as well as the negative control NIH/3T3 cell line, was detected using Fluorescent Activated Cell Scanning (FACS™) employing the LRP/LR specific antibody IgG1-iS18 coupled to FITC. The results shown in Figure 15 clearly indicate the binding of the LRP-specific antibody IgG1-iS18 to the cell surface 37kDa LRP. The shift that can be seen between the black and the gray curves indicates that a change in fluorescence intensity was detected. This shift is due to the fluorescence of the FITC that is bound to the LRP-specific antibody IgG1-iS18. FACS™ analysis revealed a 1.11 significant fold increase in LRP/LR levels on HT-1080 (88%) (Fig. 14a), in comparison to NIH/3T3 (79%) (Fig.14b). A significantly increased level of LRP/LR was noted in all neoplastic cell lines with a 1.25 fold higher level on A549 cells (98%) (Fig. 14c) and SW480 cells (99%) (Fig. 14d), a 1.223 fold higher level on HeLa cells (Fig. 14e), a 1.24 fold higher level on LNCaP (Fig. 14f), and a 1.19 fold higher level on the non-invasive MCF-7 cells (Fig.14g).

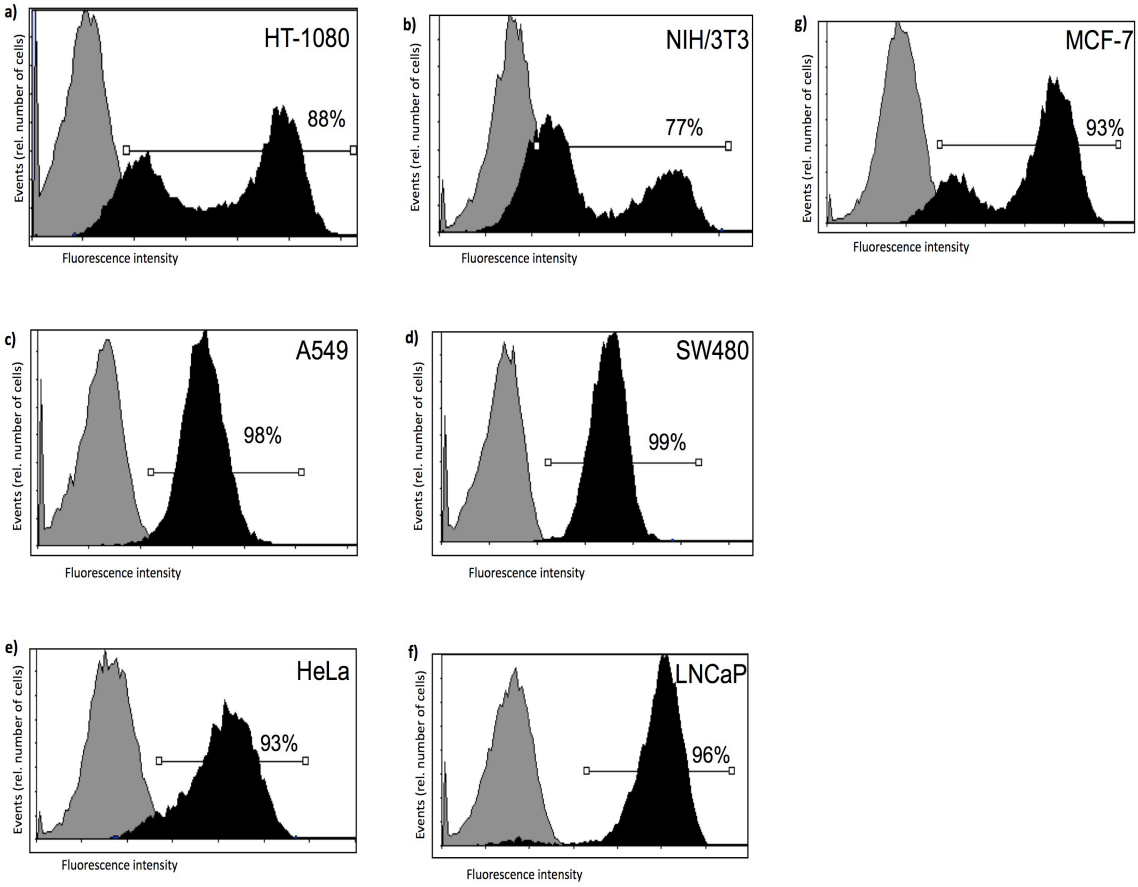


Figure 14: Detection of 37kDa/67kDa LRP/LR levels on the surface of various cell lines. Fluorescence Activated Cell Scanning (FACS™) analysis was performed using a FITC coupled IgG1-iS18 antibody on (a) HT-1080, (b) NIH/3T3, (c) A549, (d) SW480, (e) HeLa, (f) LNCaP and (g) MCF-7 cells. The gray curve represents the control with no antibody while the black curve represents the cells incubated with the fluorescence labelled antibody. Cells were not permeabilized. The double peak seen in (a), (b) and (g) could be attributed to non-specific binding with the second peak possibly indicative of some antibody binding well while others not at all. This could mean that there is a different characteristic in some of the cells of that type that causes a small percentage to bind to the fluorophore, or that there is a certain limit to the percentage of FITC-coupled antibody that can bind in any one sample.

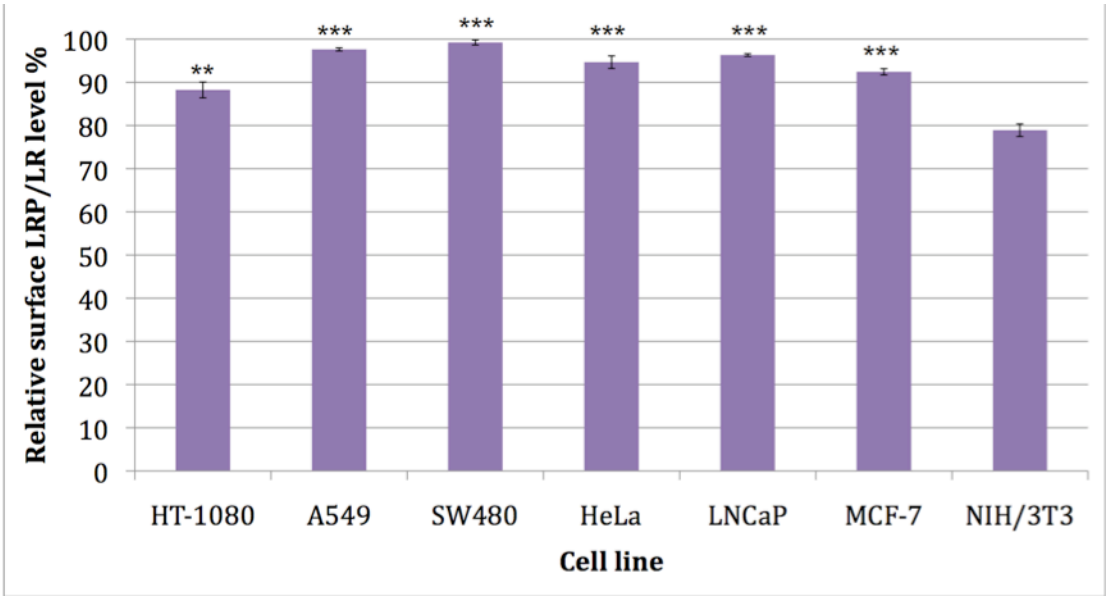


Figure 15: Bar chart of surface LRP/LR levels on HT-1080, A549, SW480, HeLa, LNCaP, MCF-7 and NIH/3T3 cells analyzed by FACS™. Neoplastic cell lines displayed significantly higher cell surface LRP/LR levels compared to NIH/3T3 cells. Data extracted from Figure 14. Data are representative of three independent experiments comprising cells from different cultures.

4.2.2 Total LRP levels

Total LRP/LR levels of neoplastic cell lines

To investigate a possible correlation between the level of LRP/LR with the invasive potential of tumorigenic cell lines, the total LRP/LR level, including cytoplasmic and cell membrane LRP/LR was determined by semi-quantitative Western Blot analysis. The protein concentration of cell lysates derived from the various cell lines was ascertained using a BCA-assay. The amount of protein loaded was standardized to 30µg of total cellular protein. Western Blot analysis was then performed and the anti-LRP/LR specific IgG1-iS18 was employed as the primary antibody with a goat anti-human POD coupled secondary antibody. As a loading control ß-actin was also employed and a rabbit anti-mouse antibody specific for ß-actin was used as the secondary antibody (see Materials and Methods). It was found that the stripping of the membrane was ineffective and therefore two different membranes were used to detect each protein. i.e. one membrane was incubated with the LRP/LR specific antibody IgG1-iS18 and the other with the mouse anti-ß-actin antibody. The 37kDa LRP was detected and the blots shown in figure 16, however, the 67kDa form could not be detected in the cell lysates using Western Blotting and the IgG1-iS18 specific antibody (Data not shown). Lysates were collected from 3 different cultures for each cell line.

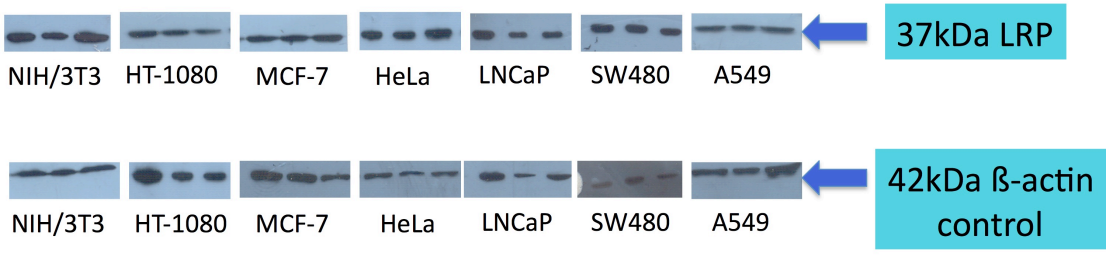


Figure 16: Analysis of the relative expression of the total LRP/LR levels in several neoplastic cell lines detected with IgG1-iS18, which binds to the 37kDa LRP and the anti-ß-actin antibody specific for the 42kDa ß-actin (acting as loading control). 30µg of total cellular protein was loaded.

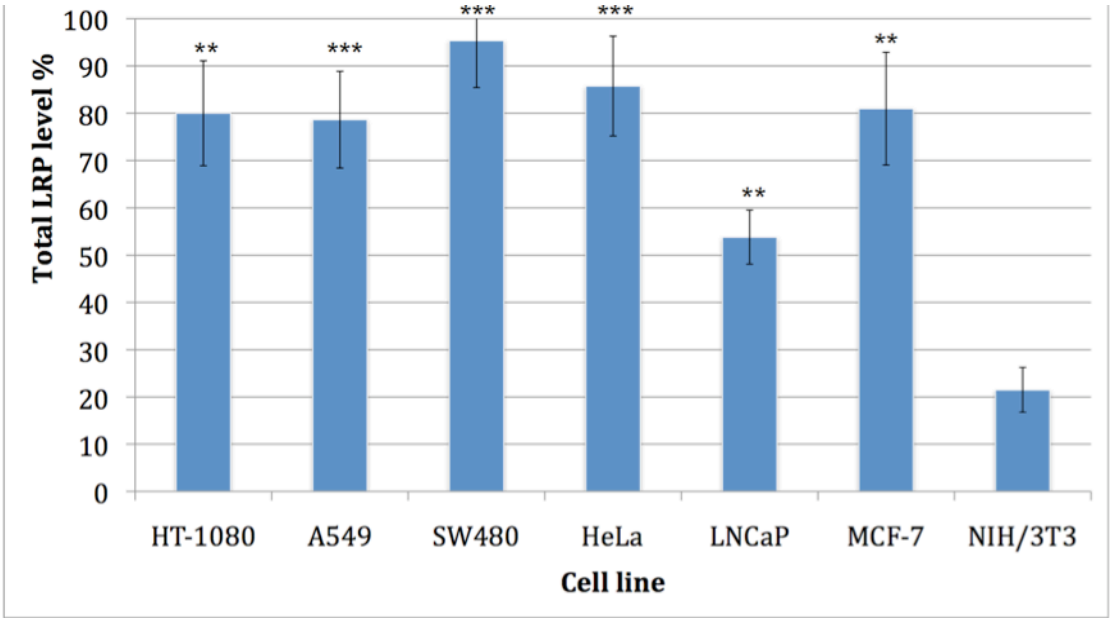


Figure 17: Graphic illustration of the relative expression of the total LRP levels of neoplastic cell lines detected by IgG1-iS18 primary antibody and goat anti-human POD secondary antibody by Western Blotting quantified using densitometry. Percentages represent the Integrated Optical Density (IOD). Each was carried out in triplicate with cells from different cultures.

As can be seen in figure 17, all neoplastic cell lines contained significantly higher levels of LRP in comparison to the non-tumorigenic control NIH/3T3 cell line. The most significant increase in total LRP levels was noted in the SW480 (human colon adenocarcinoma) cell line, concurrent with the highest cell surface LRP also noted in this cell line. Interestingly, the LNCaP (human prostate carcinoma) cell line, although showing a significant increase in LRP level in comparison to the NIH/3T3, seems to contain the least LRP amongst the neoplastic cell lines (Figure 17).

4.3 Cell adhesion potential

Neoplastic cell adhesion to Laminin-1 impeded by LRP/LR specific antibody IgG1-iS18

The adhesion to Laminin-1 is vital for the invasion of neoplastic cells. The potential of the anti-LRP/LR antibody IgG1-iS18 in the blockage of this binding was determined using adhesion assays. Neoplastic cells were incubated with IgG1-iS18 and IgG1-HD37 control antibody (0.2 µg/µl). Cells were transferred to a 96-well plate, either coated with Laminin-1 or uncoated, for 1 hour at 37°C. Optimization of these parameters was done by researching previous studies done and repeating experiments. Buffer was used in place of antibody in the no antibody control samples. Attached cells were stained and absorbance measured at 550 nm. Attachment to the uncoated plate (w/o Laminin-1 control) represents the background binding. The absorbance of the stain present correlates with the percentage of laminin-attached cells. A significantly decreased adhesion potential is noted in all neoplastic cell lines except the MCF-7 cell line (p= 0.4129), upon application of IgG1-iS18 (medium red) in comparison to the no antibody control (deep red) (Fig. 18). The control cell line, mouse embryonic fibroblasts NIH/3T3 displayed a 28% reduction in adhesion potential following incubation with IgG1-iS18 antibody (p= 0.0076). The positive control cell line HT-1080 showed a similar decrease in adhesion potential 21% (p= 0.0064). LnCap cells showed a 20% reduction (p= 0.0225) and HeLa cells a 14% reduction (p= 0.0323). The most noteworthy reduction was seen in SW480 cells with a 74% reduction (p= 0.0007) and a 48% reduction in adhesion was noted in A549 cells (p= 0.0134) (Table 10). Furthermore, the control IgG1-HD37 (light red) antibody has no significant effect on the adhesion potential ($p > 0.1663$). Data are representative of experiments carried out in triplicate.

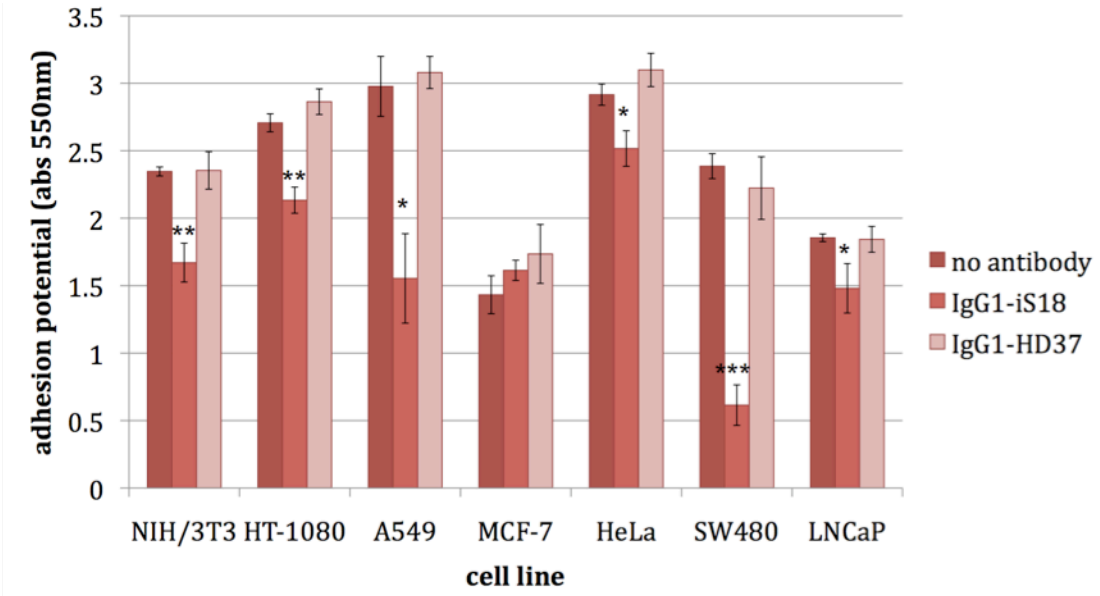


Figure 18: Adhesion to Laminin-1significantly impeded by anti-LRP/LR specific antibody IgG1-iS18 following an incubation of 1 hour on Laminin-1 coated plates at 37°C. Cells were applied on to a 96-well place, either coated with Laminin-1 or uncoated. After the attached cells were washed, they were stained with crystal violet and absorbance measured at 570nm. Cells attached to uncoated wells represent the background binding.

Table 10: Percentage reduction in adhesion potential in various neoplastic cell lines

Cell line	**% Reduction in adhesion potential**	***P*- value**
HT-1080	21%	0.0064 **
A549	48%	0.0134 *
MCF-7	0%	0.1540
HeLa	14%	0.0323 *
SW480	74%	0.0007 ***
LNCaP	20%	0.0225 *

Note: the % in reduction in adhesion potential refers to the difference in adhesion potential between the samples without antibody compared to cells incubated with IgG1-iS18 antibody.
P-values calculated using two-tailed Students t-test with a 95% confidence interval. Please refer to 3.8 for details of statistical evaluation.

4.4 Invasive potential

4.4.1 Determination of cell invasive potential of selected neoplastic cell lines

Prior to investigating the effect of LRP/LR specific antibodies on the invasive potential, we had to determine the invasive potential of the neoplastic cell lines HT-1080, A549, HeLa, SW480 and LNCaP. These particular cell lines were chosen as they are described as having an invasive potential. The non-invasive MCF-7 cell line served as a negative control since it is known to be non-invasive[53]. Even in the presence of a chemo-attractant the MCF-7 cells did not invade the Matrigel™, therefore the extent to which the other neoplastic cells had invaded was compared to the MCF-7 cell line and the statistical evaluation was done in accordance with this. In previous studies, the tumorigenic fibrosarcoma cell line HT-1080 was analyzed and its invasive potential determined to be greater than that of the non-tumorigenic mouse embryonic fibroblast cell line NIH/3T3[33]. This study confirmed that the HT-1080 are in fact invasive following an 18 hour incubation on a polymerized Matrigel™. HT-1080 cells showed a significantly increased in the invasive potential of 78% in comparison to the MCF-7 cell line ($p= 0.0001$). The A549 and HeLa cells displayed a similar trend with increased invasive potentials of 83% and 85%, respectively ($p= 0.0001$). In the same experimental setup, LNCaP was also found to be significantly more invasive than the MCF-7 cell line with a 82% increase, however the most invasive of the neoplastic cell lines was the SW480 (human colon adenocarcinoma) cell line with a 86% increased invasive potential ($p = 0.0001$) (Figure 19) (Table 11).

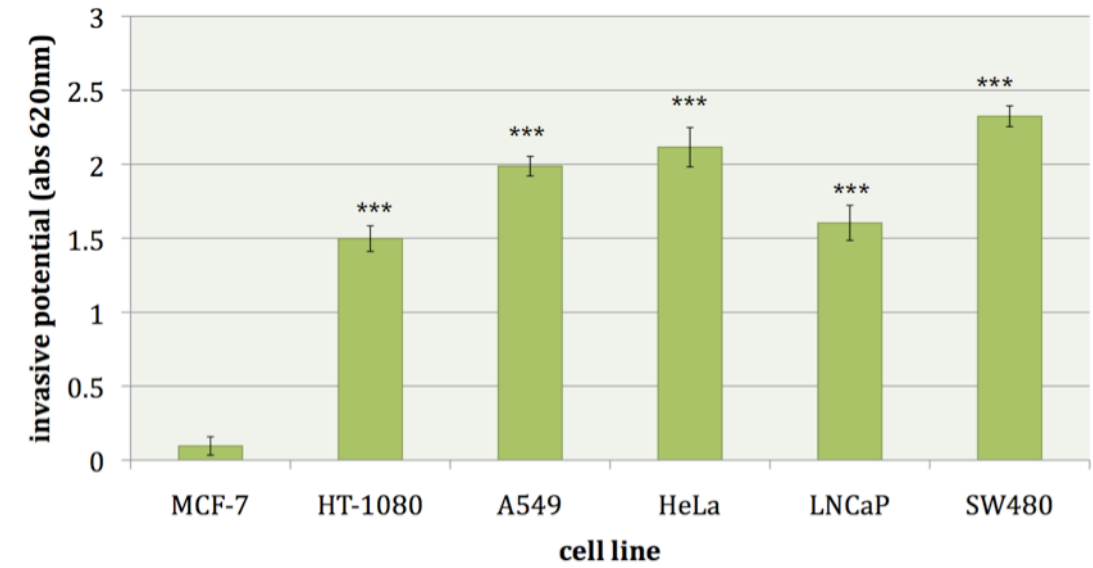


Figure 19: Tumorigenic cells reveal a significantly increased invasive potential in comparison to non-invasive MCF-7 cells after 18 hour incubation on a polymerized Matrigel™ at 37°C, 5% CO_2. The absorption of invaded cells stained with toluidine blue was measured at 620nm.

Table 11: Tumorigenic cell lines with their invasive behaviour and invasive potential relative to the MCF-7 cell line

Cell line	Cell type	Invasive potential	% Invasive potential relative to MCF-7
MCF-7	Human breast adenocarcinoma cells	Non-invasive	-
HT-1080	Human fibrosarcoma cells	Invasive	60%
A549	Human lung carcinoma cells	Invasive	81%
HeLa	Human cervix carcinoma cells	Invasive	86%
LNCaP	Human prostate carcinoma cells	Invasive	65%
SW480	Human colon adenocarcinoma cells	Invasive	95%

Note: Invasive potentials were determined using the absorbance measured at 620nm. A percentage was then determined by calculating the difference between the respective cell line and the invasive potential value of MCF-7 and then dividing by the highest value (SW480 set to 100%).

4.4.2 IgG1-iS18 significantly decreased the invasive potential in neoplastic cell lines

Invasion assays were performed using the aforementioned neoplastic cell lines and the ability of the IgG1-iS18 antibody in hindering cell invasion was determined. These cell lines were pre-incubated with 0.2µg/µl of the full-length anti-LRP/LR specific antibody IgG1-iS18 and the anti-CD19 control antibody IgG1-HD37. Once again the invasive potentials of cells that were not pre-incubated with antibody was determined as in 5.4.1 ensure accuracy and show if the control antibody had an effect on invasion. It was found that the invasive potential of the HT-1080 cells in the absence of antibody did not differ significantly to those of the HT-1080 cells incubated with the control antibody IgG1-HD37 (p = 0.1520). A significant decrease in invasion of 44% was noted in HT-1080 cells upon application of the IgG1-iS18 antibody when compared to the sample containing no antibody (p= 0.0030) (Figure 20). A549 cell invasion was impeded significantly by 33% (p = 0.0127) with the use of IgG1-iS18 in contrast to the no antibody control. In comparison to the no antibody sample the means of the control antibody IgG1-HD37 did not differ significantly (p = 0.5495) in A549 cells (Fig. 22). A similar trend was seen with HeLa cells with a very significant reduction of 57% in the invasion following incubation with the IgG1-iS18 antibody (p = 0.0002) in comparison to the sample containing no antibody (Fig. 21). Invasion was significantly hindered by 38% after pre-incubation of LNCaP cells with the anti-LRP/LR antibody in comparison to the no antibody control as well the IgG1-HD37 control (p = 0.0003) (Fig. 23). The most significant decrease in invasion potential upon application of IgG1-iS18 was seen in SW480 cells demonstrating a 91% reduction (p = 0.0001) (Fig. 24), with invasive behaviour remaining unaffected by the negative control antibody. Overall, it was observed that the anti-LRP/LR antibody significantly reduced the invasive capability in the various neoplastic cell lines (Table 12). Representative photographs clearly illustrated the decrease in the amount of toluidine blue stain that was retained by cells that had invaded (Figure 25).

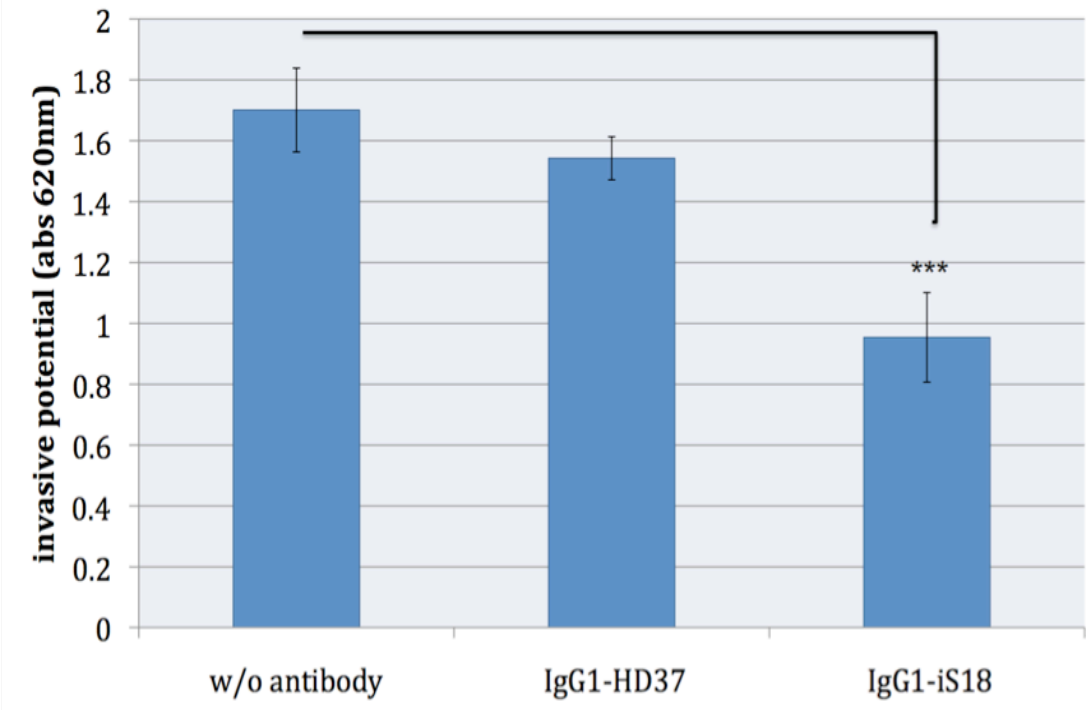


Figure 20: Decreased invasive potential of HT-1080 human fibrosarcoma cells by 0.2µg/µl of IgG1-iS18 after a 10 minute pre-incubation with the antibodies and 18 incubation on the polymerized Matrigel™ at 37°C, 5% CO_2. The stain retained by invaded cells was extracted and measured at 620nm. Background invasion was deducted.

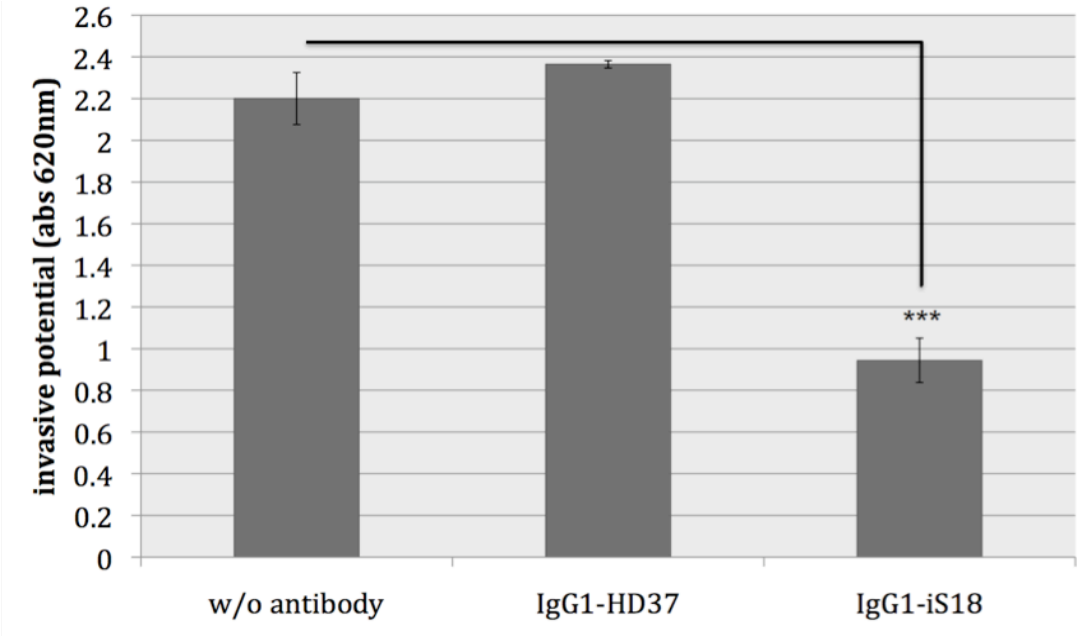


Figure 21: Decreased invasive potential of HeLa human cervix carcinoma cells by 0.2µg/µl of IgG1-iS18 after a 10 minute pre-incubation with the antibodies and 18 incubation on the polymerized Matrigel™ at 37°C, 5% CO_2. The stain retained by invaded cells was extracted and measured at 620nm. Background invasion was deducted.

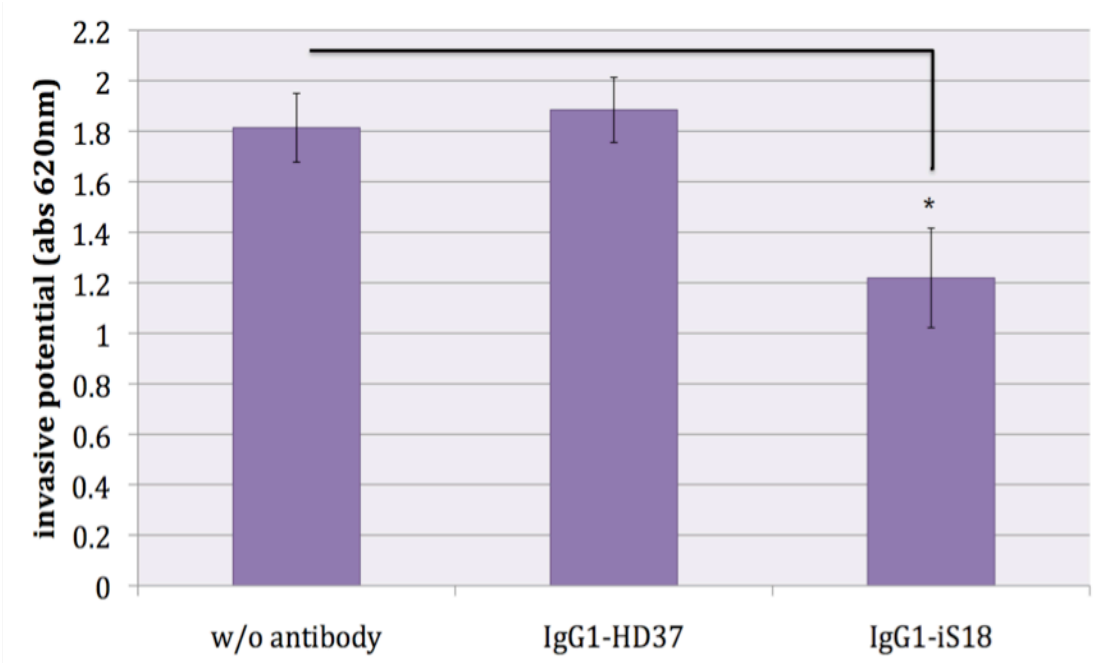


Figure 22: Decreased invasive potential of A549 human lung carcinoma cells by 0.2µg/µl of IgG1-iS18 after a 10 minute pre-incubation with the antibodies and 18 incubation on the polymerized Matrigel™ at 37°C, 5% CO_2. The stain retained by invaded cells was extracted and measured at 620nm. Background invasion was deducted.

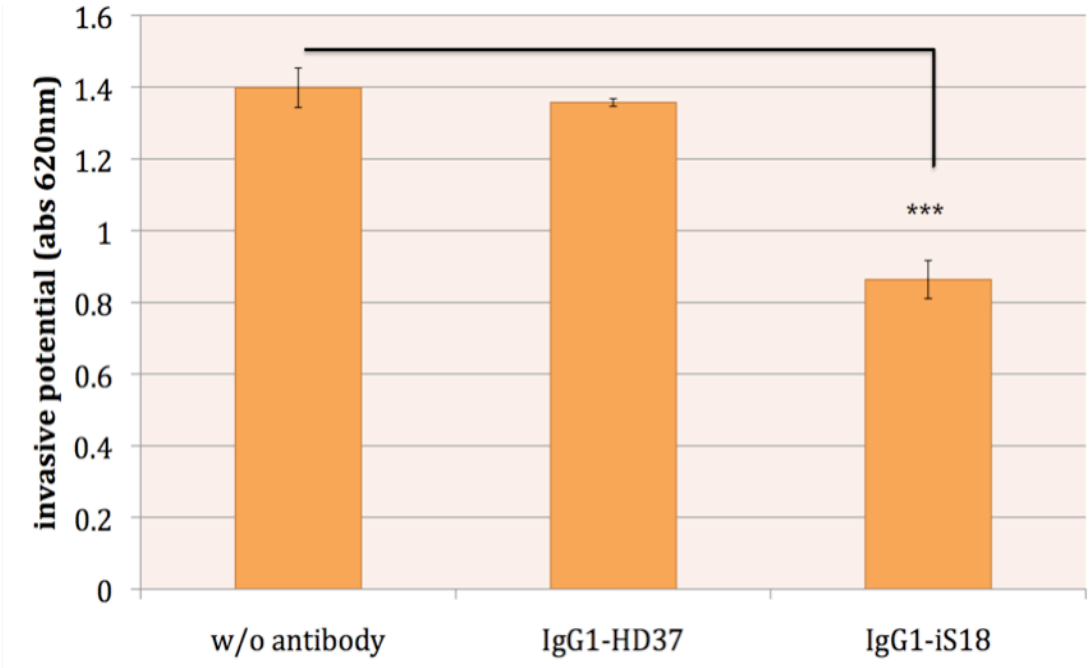


Figure 23: Decreased invasive potential of LNCaP human prostate carcinoma cells by 0.2µg/µl of IgG1-iS18 after a 10 minute pre-incubation with the antibodies and 18 incubation on the polymerized Matrigel™ at 37°C, 5% CO_2. The stain retained by invaded cells was extracted and measured at 620nm. Background invasion was deducted.

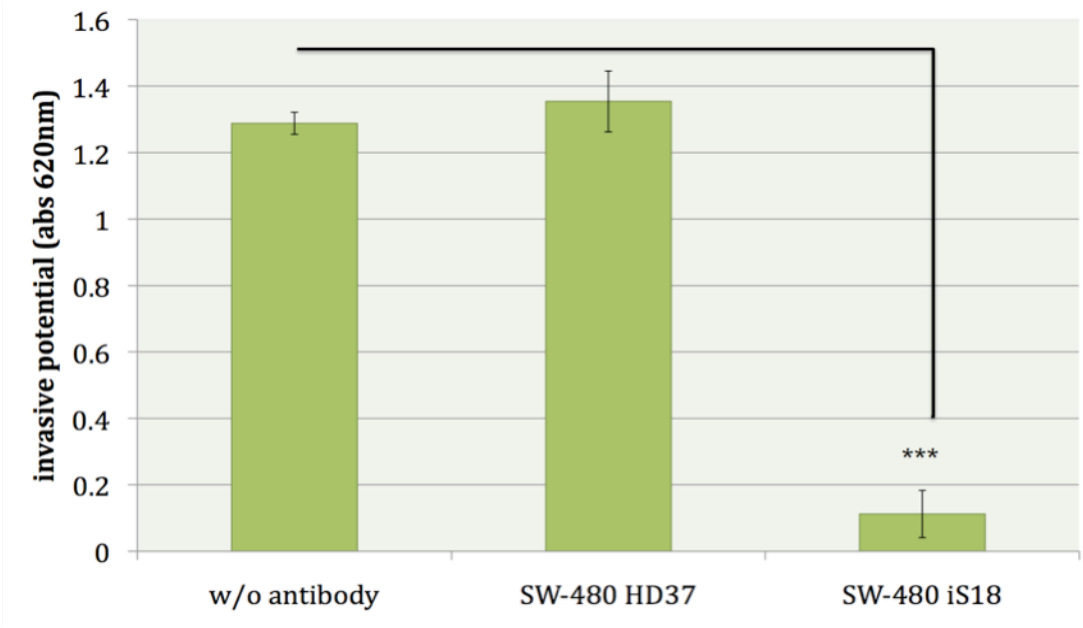


Figure 24: Decreased invasive potential of SW480 human colon adenocarcinoma cells by 0.2µg/µl of IgG1-iS18 after a 10 minute pre-incubation with the antibodies and 18 incubation on the polymerized Matrigel™ at 37°C, 5% CO_2. The stain retained by invaded cells was extracted and measured at 620nm. Background invasion was deducted.

Table 12: Invasion into Matrigel™ matrix is significantly impeded by IgG1-iS18 antibody

Cell line:	% Reduction in invasion	*P*-value
HT-1080	44%	0.0030 ***
HeLa	57%	0.0002 ***
A549	33%	0.0127 *
LNCaP	38%	0.0003 ***
SW480	91%	0.0001 ***

Note: The % reduction in invasion is the difference in invasive potential between cells without antibody compared to cells incubated with IgG1-iS18 antibody.
P-values calculated using two-tailed Students *t*-test with a 95% confidence interval.
Please refer to 3.8 for details of statistical evaluation.

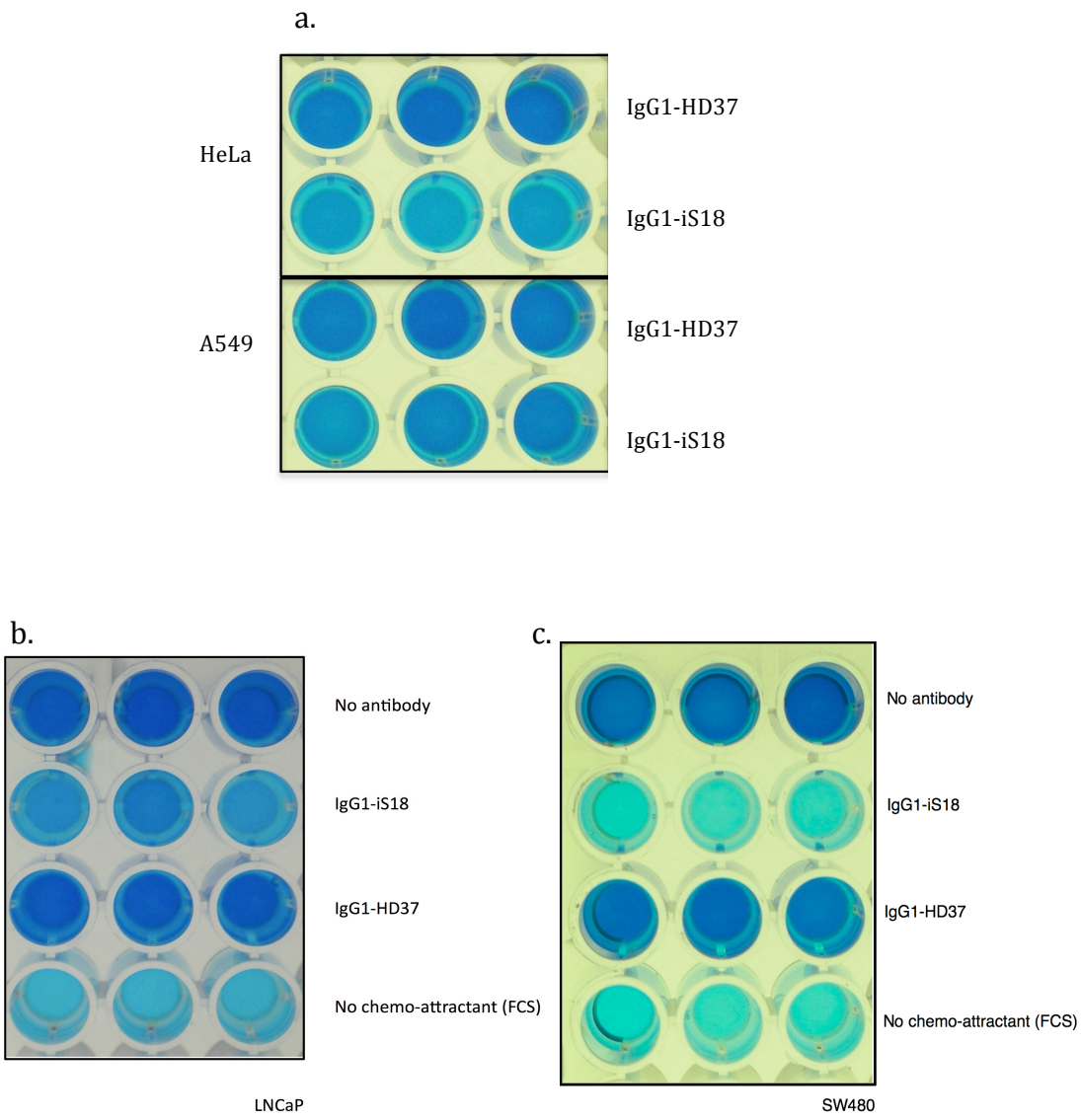


Figure 25: Cell invasion through a Matrigel™ matrix is inhibited by anti-LRP specific antibody IgG1-iS18. Representative photographs of invaded cells stained toluidine blue. These images were taken after the dye was extracted from cells and the absorbance of this was then measured at 620nm. The staining correlates with the number of cells that was able to invade. a.) As can be seen from the shade of blue, the IgG1-iS18 incubated cells had an impaired ability to invade in both the HeLa and A549 cell lines. (lighter blue). b.) A similar observation was made with the LNCaP cell line and c.) SW480 cell line where there is a distinct difference in the amount of dye present and therefore fewer invaded cells upon application of IgG1-iS18.

CHAPTER FIVE – DISCUSSION

In this study we examined the effect of the anti-LRP/LR specific antibody IgG1-iS18 on cell invasion and cell adhesion in various neoplastic cell lines in order to ascertain its potential as a therapeutic tool for the treatment of metastatic cancer. For this to be achieved, the full-length IgG1-iS18 antibody and the control antibody IgG1-HD37 were initially produced by the over-expression in a mammalian cell system and then characterized by Western Blotting analysis. The antibody was then applied in subsequent assays with additional antibody kindly supplied by Affimed Therapeutics.

5.1 Antibody development

Monoclonal antibodies (MAb's) currently represent over 30% of biopharmaceuticals used in clinical trials and approximately 60-70% of all pharmaceuticals based on recombinant protein are produced in mammalian cell systems[54]. HEK293 (human embryonic kidney) cells, and other cultivated mammalian systems, have become preferred choices for the production of recombinant proteins for clinical application due their ability to allow for correct protein folding, assembly and post-translational modifications. Further advances in this specific system include the HEK293 cells being stably transfected with the EBNA-1 gene, which enhances the protein expression when the plasmid DNA contains EBV oriP. Particularly, in the last decade, immunotherapy has received immense attention, however, in some instances monoclonal antibodies have limited application in human clinical trials due to their immunogenicity. With the use of modern genetic engineering techniques we are now able to produce chimeric mouse/human as well as completely human antibodies[55]. The development of single-chain antibodies, which are composed of variable regions of the heavy and light chains joined by a short peptide linker, were found to have a short half-life of approximately 12 hours in the blood. In order to overcome this limitation of the scFv, full-length antibodies were created by Affimed Therapeutics Heidelberg. Apart from the longer half-life, these enhanced full-length antibodies have a higher affinity for LRP/LR combined with the avid effect caused by bivalent binding.

5.2 Process of metastasis

In order for tumor metastasis to occur the cells comprising the primary tumor must first acquire the ability to proteolyse the ECM, concomitant with the breakage of existing attachments, thereafter the extension of pseudopodia as well as translocation will result in these cells entering the circulatory system. The final step in the process is the invasion and colonization of distant organ sites[56]. The hypothesis that the metastatic potential of tumor cells correlates with enzymatic degradation of the basement membrane type IV collagen is supported by several studies[57].

Crossing of the basement membrane by neoplastic cells is a vital step in the process of metastasis[41]. As a major basement membrane glycoprotein, Laminin-1 plays a crucial role in cell attachment, migration, proliferation, growth and differentiation, elucidating its function in tumor invasion and metastasis. *In vitro* as well as *in vivo* studies have demonstrated that the attachment of tumor cells to Laminin-1 augments tumorigenic and metastatic potential[58]. The 37kDa/67kDa LRP/LR receptor was first isolated from tumor cells[36] and since has been found to be over-expressed in several cancer cell lines[58]. The receptor is thought to play a crucial role during cell invasion and therefore in the metastasis due to its interaction with Laminin-1[41] and consequently the degradation of the basement membrane.

5.3 LRP/LR, cell surface LRP and total LRP levels

A full-length gene encodes for the 37kDa Laminin Receptor Precursor. To date, it is unknown how the 67kDa LR originates from the 37kDa LRP[3]. Although LRP/LR is a non-integrin receptor it acts as an integrin-accessory molecule by stabilizing the binding of laminin to cell surface integrins. Due to this involvement with integrins, which are the primary mediators of cell adhesion, the potential effect that blocking LRP/LR could have is quite evident. Integrins also play a role in signal transduction to the nucleus following interactions between cells as well as cell-ECM interactions[36]. Perhaps, the anti-LRP/LR specific antibody impedes this process resulting in a decreased adhesion potential.

LRP/LR offers two binding sites for Laminin-1, a peptide G sequence (aa 161-180) and another at the carboxy terminus (aa 205-229)[3]. Due to LRP spanning the lipid bilayer as well as having the C-terminus situated in the extracellular space and a cytoplasmic N-terminus, it can be classified as a type II transmembrane protein. Both the laminin binding domains are found in the extracellular space where[3], upon interaction with Laminin-1, it boosts tumor cell invasion and aggressiveness, induces further expression of the 67kDa LR as well as activates proteolytic enzymes that consequently lead to extracellular matrix degradation[38]. The interaction between the 67kDa form and Laminin-1 causes the up-regulation of various processes that ultimately results in an enhanced ability to invade distal tissue via the hematogenous route. An increased expression of the 67kDa form in conjunction with the further activation of proteolytic enzymes contributes to this enhancement[33].

The level of LRP/LR on the surface of these cell lines was ascertained using FACS™ analysis in order to determine the degree of correlation between LRP/LR levels and invasion and adhesion potential. FACS™ analysis revealed that HT-1080 cells have increased cell surface levels of LRP/LR in comparison to NIH/3T3 with a 1.1 fold higher level, confirming findings of previous studies[33]. The control mouse embryonic fibroblasts (NIH/3T3) have a decreased invasive potential when compared to the human fibrosarcoma cell line (HT-1080). This result was expected since NIH/3T3 cells are known to be non-tumorigenic and non-invasive[59]. All neoplastic cell lines displayed significantly higher levels of cell surface LRP/LR including the non-invasive MCF-7 cell line. The greatest increase in LRP/LR levels was found in A549 and SW480 cells. Furthermore, not only did the SW480 cells reveal significantly increased levels of LRP/LR, they also proved to have the highest invasive potential. By calculating the Pearson's correlation co-efficient between the levels of LRP/LR and the respective invasive potentials, it was found to be 0.53 (Table 13), indicating that the correlation is positive thus there is a positive relationship. Therefore, we propose that in most instances a higher LRP/LR level correlates with an increased invasive potential.

Table 13: Pearson's correlation coefficient values

LRP/LR levels correlation to invasive potential	Invasive potential correlation to adhesion potential
0.53 positive	0.77 positive

5.4 Surface and total LRP levels appear not to be an accurate indication of invasive potential

Despite a correlation between cell surface LRP/LR levels and invasive potential, this is not always the case since the MCF-7 cell line is an exception. Interestingly, with a relatively high cell surface LRP level illustrated by FACS™ analysis (93%), and total LRP/LR level demonstrated using Western Blotting (81%), it was found to have an extremely low and almost undetectable invasive potential. The MCF-7 breast carcinoma cell line was established from the pleural effusion of a patient with breast adenocarcinoma[60] and was found to contain estrogen receptors. A possible explanation for the unexpected behavior displayed in this study could be that these cells require estrogens to proceed with invasion and thereby express a great malignant character[61]. Studies have shown that 17ß-estradiol is able to stimulate the invasive and metastatic potential of tumorigenic cells. Traversing though an artificially synthesized basement membrane in vitro was also enhanced[62], and this trend was also demonstrated in nude mice upon which the introduction of 17ß-estradiol resulted in increased tumor formation as well as distant metastasis[63].

5.5 Optimizing invasion assay

Manipulation of the Matrigel™ matrix concentration, polymerization times, as well as the duration of incubation of cells on the matrix was well achieved and experiments were done prior to the actual study in order to optimize these parameters. It was found that the most suitable concentration of Matrigel™ was 1mg/ml, a polymerization time of 6 hours and an incubation time of 18 hours was ideal. A way in which the invasion assay could be improved further is with the use of Growth Factor Reduced Matrigel™ Matrix. This form of Matrigel™ is purified and characterized to a greater extent than the Matrigel™ used in this study. It contains a reduced the level of a variety of growth factors except for TGF-beta which may be bound to collagen IV. The major components of Matrigel™, such as laminin, collagen IV and entactin (nidogen) are

conserved by the purification process, however the level of heparan sulfate proteoglycan is reduced by 40-50%.

5.6 Effect of IgG1-iS18 antibody on invasion and adhesion

The Pearson's correlation co-efficient of the adhesion potential and the invasion potential was found to be 0.77 (Table 13), indicating a definite positive relationship, further proving that adhesion is a pre-requisite for invasion. The results presented in this study clearly indicate the considerable decrease in adhesion potential in important cancer types following incubation with the anti-LRP/LR specific antibody. A reduction of up to 74% in adhesion potential was observed in SW480 cells and a noteworthy 48% decline in A-549 cells, respectively. The significant effect of the IgG1-iS18 antibody on the invasion potential can be attributed to changes on a molecular level, which include the blockage of adhesion. Application of IgG1-iS18 had a significant effect on 5 major cancer types concomitant with a reduction in the invasive potential. A remarkable decrease of 91% of the invasive potential of SW480 cells and a convincing reduction of 57% invasive potential in HeLa cells opens new possibilities of hindering the invasion of neoplastic cells. The molecular mechanisms underlying blockage of invasion includes the blockage of adhesion. The significant reduction in invasion and adhesion of human fibrosarcoma (HT-1080), human cervix carcinoma (HeLa), human lung carcinoma (A549), human prostrate carcinoma (LNCaP) and human colon adenocarcinoma (SW480), by the antibody IgG1-iS18 suggest that this macromolecule might act as a therapeutic tool for the treatment of many metastatic cancer types targeting the Laminin-1 and LRP/LR interaction.

Previous studies demonstrated that the application of anti-LRP/LR tools resulted in the significant hindrance of invasive potential of human fibrosarcoma (HT-1080) cells. siRNA's directed against LRP mRNA achieved a significant reduction in invasion by 37%[33]. Moreover, other approaches that included the pentosan polysulfate SP-54 as well as the heparan mimetic HM2602, significantly blocked the invasion of HT-1080 cells by 35% and 20% respectively[33]. In the same study it was found that the single chain antibody scFv iS18 was able to reduce invasion by 37% and that the full-length antibody IgG1-iS18, that was the focus of this study, displayed a 38% reduction in invasion[33]. The reduced invasive behavior of human fibrosarcoma

cells (HT-1080) noted due to application of anti-LRP/LR tools, in conjunction with the cell adhesion assay results were analyzed. It was proposed that this impaired invasive potential could be attributed to the obstruction of the adhesion of LRP/LR (expressed on the cell surface) to Laminin-1.

5.7 Antibody activity

It has also been suggested that the binding of the IgG1-iS18 antibody to LRP/LR may influence the Mitogen-Activated Protein Kinase (MAPK) signaling cascade since it is induced by an interaction with Laminin-1. Serine and threonine are particular protein kinases of interest due to their influential role in tumor metastasis. Other possible mechanisms by which the anti-LRPL/LR specific antibody IgG1-iS18 functions could be by the sterical blockage of either one or both of the laminin binding sites situated at aa161-180 and aa205-229 Figure 3. The same effect could be achieved by directly occupying these laminin-binding sites, however, the exact mechanism of the antibody action is yet to be elucidated.

In the present study, tumorigenic cell lines incubated with the anti-LRP/LR antibody IgG1-iS18 demonstrated a significantly decreased ability to attach to Laminin-1 and to traverse Matrigel™ coated inserts. These findings are in agreement with other studies elucidating the role of the 67kDa laminin receptor in attachment to Laminin-1 and invasion of tumor cells[33].

5.8 Outlook

Matrigel™ is a heterogenous composition that can be used to simulate the basement membrane since it is prepared from solubilized basement membrane extracted from Engelbreth-Holm-Swarm (EHS) mouse sarcoma cells. This cell line is ideal since it is known to be rich in extracellular matrix proteins such as laminin, collagen IV, heparan sulfate proteoglycans and entactin[64]. Several other compounds that occur naturally in the EHS tumor include TGF-ß, epidermal growth factor, insulin-like growth factor, fibroblast growth factor and tissue plasminogen activator[65]. Matrigel™ also contains various other proteins and although present in low concentrations they could possibly influence the results obtained. Overall the exact composition of the matrix is not provided and only a total protein concentration is given (10mg/ml),

therefore, the amount of laminin present is unknown and could vary between batches. In this study, the batch of Matrigel™ was consistent throughout the many invasion assays, however results could differ if experiments were to be repeated with a different batch due to the varying concentrations of ECM proteins. Alternatives to a Matrigel™ Matrix include chicken chorioallantoic membrane, mouse urinary bladder, human amnion, other placental membranes and lens capsule of the eye[66]. Perhaps further studies could be done using other matrices derived from these sources to confirm results; also, the exact composition of the matrix should be determined to ensure accuracy, in particular the concentration of laminin.

Seeing as only the 5 major cancer types were used in this study, it would be interesting to apply the anti-LRP/LR specific antibody to other cancer types, such as liver, pancreatic, gastric and invasive breast cancer combating the top ten cancer types worldwide.

Since the anti-LRP/LR specific antibody IgG1-iS18 was able to significantly reduce adhesion and invasion in vitro, and is also known to have a half-life of approximately 3 weeks in blood, it serves as a viable option a therapeutic to be tested *in vivo*. Currently several mouse models are available, using A549 human lung carcinoma cells and HT-1080 human fibrosarcoma cells to induce tumors and metastasis formation[67]. Also, a mouse model bearing human prostate cancer in which the tumorigenic cells were inoculated under the skin has been used to demonstrate the anti-tumor effect of siRNA's[68]. There have been claims that transgenic tumor models, or subcutaneously growing human tumors induced in immuno-deficient mice cannot be a precise representation of clinical cancer, and therefore does not accurately display metastatic activity and cannot be used to assess drug sensitivity efficiently. Alternatives such as orthotopic implantations allow for the direct transplantation of fragments of intact human tumors into the equivalent organ in immuno-deficient mice and therefore represents clinical cancer[69]. These models in conjunction with *in vivo* imaging technology serve as a bridge linking pre-clinical and clinical research and drug development, allowing for effective testing of potential anti-metastatic therapies including the anti-LRP/LR specific antibody IgG1-iS18.

6. REFERENCES

1. Guinn, B.A. & Mulherkar, R. International progress in cancer gene therapy. *Cancer Gene Therapy* **15**, 765-775 (2008).
2. Shay, J.W. Meeting report: the role of telomeres and telomerase in cancer. *Cancer Res* **65**, 3513-3517 (2005).
3. Mbazima, V., Da Costa Dias, B., Omar, A., Jovanovic, K. & Weiss, S.F. Interactions between PrP(c) and other ligands with the 37-kDa/67-kDa laminin receptor. *Front Biosci* **15**, 1150-1163.
4. Hanahan, D. & Weinberg, R.A. The hallmarks of cancer. *Cell* **100**, 57-70 (2000).
5. Susantad, T. & Smith, D.R. siRNA-mediated silencing of the 37/67-kDa high affinity laminin receptor in Hep3B cells induces apoptosis. *Cell Mol Biol Lett* **13**, 452-464 (2008).
6. Malinda, K.M. & Kleinman, H.K. The laminins. *Int J Biochem Cell Biol* **28**, 957-959 (1996).
7. Malinda, K.M.*, et al.* Identification of laminin alpha1 and beta1 chain peptides active for endothelial cell adhesion, tube formation, and aortic sprouting. *FASEB J* **13**, 53-62 (1999).
8. Aznavoorian, S., Stracke, M.L., Krutzsch, H., Schiffmann, E. & Liotta, L.A. Signal transduction for chemotaxis and haptotaxis by matrix molecules in tumor cells. *J Cell Biol* **110**, 1427-1438 (1990).
9. Giancotti, F.G. Signal transduction by the alpha 6 beta 4 integrin: charting the path between laminin binding and nuclear events. *J Cell Sci* **109 (Pt 6)**, 1165-1172 (1996).
10. Kibbey, M.C., Grant, D.S. & Kleinman, H.K. Role of the SIKVAV site of laminin in promotion of angiogenesis and tumor growth: an in vivo Matrigel model. *J Natl Cancer Inst* **84**, 1633-1638 (1992).
11. Vana, K.*, et al.* LRP/LR as an alternative promising target in therapy of prion diseases, Alzheimer's disease and cancer. *Infect Disord Drug Targets* **9**, 69-80 (2009).
12. Zuber, C.*, et al.* Delivery of single-chain antibodies (scFvs) directed against the 37/67 kDa laminin receptor into mice via recombinant adeno-associated viral vectors for prion disease gene therapy. *J Gen Virol* **89**, 2055-2061 (2008).

13. Fontanini, G.*, et al.* 67-Kilodalton laminin receptor expression correlates with worse prognostic indicators in non-small cell lung carcinomas. *Clin Cancer Res* **3**, 227-231 (1997).
14. Gauczynski, S.*, et al.* The 37-kDa/67-kDa laminin receptor acts as the cell-surface receptor for the cellular prion protein. *EMBO J* **20**, 5863-5875 (2001).
15. Gauczynski, S.*, et al.* The 37-kDa/67-kDa laminin receptor acts as a receptor for infectious prions and is inhibited by polysulfated glycanes. *J Infect Dis* **194**, 702-709 (2006).
16. Ludewigs, H.*, et al.* Therapeutic approaches for prion disorders. *Expert Rev Anti Infect Ther* **5**, 613-630 (2007).
17. Wang, K.S., Kuhn, R.J., Strauss, E.G., Ou, S. & Strauss, J.H. High-affinity laminin receptor is a receptor for Sindbis virus in mammalian cells. *J Virol* **66**, 4992-5001 (1992).
18. Akache, B.*, et al.* The 37/67-kilodalton laminin receptor is a receptor for adeno-associated virus serotypes 8, 2, 3, and 9. *J Virol* **80**, 9831-9836 (2006).
19. Ardini, E.*, et al.* The 67-kDa laminin receptor originated from a ribosomal protein that acquired a dual function during evolution. *Mol Biol Evol* **15**, 1017-1025 (1998).
20. Wewer, U.M., Taraboletti, G., Sobel, M.E., Albrechtsen, R. & Liotta, L.A. Role of laminin receptor in tumor cell migration. *Cancer Res* **47**, 5691-5698 (1987).
21. Montuori, N.*, et al.* Expression of the 67-kDa laminin receptor in acute myeloid leukemia cells mediates adhesion to laminin and is frequently associated with monocytic differentiation. *Clin Cancer Res* **5**, 1465-1472 (1999).
22. de Manzoni, G.*, et al.* Prognostic significance of 67-kDa laminin receptor expression in advanced gastric cancer. *Oncology* **55**, 456-460 (1998).
23. Cioce, V.*, et al.* Increased expression of the laminin receptor in human colon cancer. *J Natl Cancer Inst* **83**, 29-36 (1991).
24. Sanjuan, X.*, et al.* Overexpression of the 67-kD laminin receptor correlates with tumour progression in human colorectal carcinoma. *J Pathol* **179**, 376-380 (1996).
25. al-Saleh, W.*, et al.* Expression of the 67 KD laminin receptor in human cervical preneoplastic and neoplastic squamous epithelial lesions: an immunohistochemical study. *J Pathol* **181**, 287-293 (1997).
26. Nadji, M., Nassiri, M., Fresno, M., Terzian, E. & Morales, A.R. Laminin receptor in lymph node negative breast carcinoma. *Cancer* **85**, 432-436 (1999).

27. van den Brule, F.A.*, et al.* Differential expression of the 67-kD laminin receptor and 31-kD human laminin-binding protein in human ovarian carcinomas. *Eur J Cancer* **30A**, 1096-1099 (1994).
28. Pelosi, G.*, et al.* High-affinity monomeric 67-kD laminin receptors and prognosis in pancreatic endocrine tumours. *J Pathol* **183**, 62-69 (1997).
29. Waltregny, D., de Leval, L., Menard, S., de Leval, J. & Castronovo, V. Independent prognostic value of the 67-kd laminin receptor in human prostate cancer. *J Natl Cancer Inst* **89**, 1224-1227 (1997).
30. Gasparini, G.*, et al.* 67-kDa laminin-receptor expression adds prognostic information to intra-tumoral microvessel density in node-negative breast cancer. *Int J Cancer* **60**, 604-610 (1995).
31. Menard, S., Tagliabue, E. & Colnaghi, M.I. The 67 kDa laminin receptor as a prognostic factor in human cancer. *Breast Cancer Res Treat* **52**, 137-145 (1998).
32. Narumi, K.*, et al.* Inhibition of experimental metastasis of human fibrosarcoma cells by anti-recombinant 37-kDa laminin binding protein antibody. *Jpn J Cancer Res* **90**, 425-431 (1999).
33. Zuber, C.*, et al.* Invasion of tumorigenic HT1080 cells is impeded by blocking or downregulating the 37-kDa/67-kDa laminin receptor. *J Mol Biol* **378**, 530-539 (2008).
34. Tanaka, M.*, et al.* Expression of the 37-kDa laminin binding protein in murine lung tumor cell correlates with tumor angiogenesis. *Cancer Lett* **153**, 161-168 (2000).
35. Vande Broek, I.*, et al.* Laminin-1-induced migration of multiple myeloma cells involves the high-affinity 67 kD laminin receptor. *Br J Cancer* **85**, 1387-1395 (2001).
36. Menard, S., Castronovo, V., Tagliabue, E. & Sobel, M.E. New insights into the metastasis-associated 67 kD laminin receptor. *J Cell Biochem* **67**, 155-165 (1997).
37. Qiu, J.*, et al.* Occurrence of autoantibodies to annexin I, 14-3-3 theta and LAMR1 in prediagnostic lung cancer sera. *J Clin Oncol* **26**, 5060-5066 (2008).
38. Berno, V.*, et al.* The 67 kDa laminin receptor increases tumor aggressiveness by remodeling laminin-1. *Endocr Relat Cancer* **12**, 393-406 (2005).
39. Ardini, E.*, et al.* Identification of a novel function for 67-kDa laminin receptor: increase in laminin degradation rate and release of motility fragments. *Cancer Res* **62**, 1321-1325 (2002).
40. Klein, C.A. Cancer. The metastasis cascade. *Science* **321**, 1785-1787 (2008).

41. Omar, A.*, et al.* Patented biological approaches for the therapeutic modulation of the 37 kDa/67 kDa laminin receptor. *Expert Opin Ther Pat* **21**, 35-53.
42. Zuber, C., Ludewigs, H. & Weiss, S. Therapeutic approaches targeting the prion receptor LRP/LR. *Vet Microbiol* **123**, 387-393 (2007).
43. Kohler, G. & Milstein, C. Continuous cultures of fused cells secreting antibody of predefined specificity. 1975. *J Immunol* **174**, 2453-2455 (2005).
44. Skerra, A., Pfitzinger, I. & Pluckthun, A. The functional expression of antibody Fv fragments in Escherichia coli: improved vectors and a generally applicable purification technique. *Biotechnology (N Y)* **9**, 273-278 (1991).
45. Vogel, C.*, et al.* First-line, single-agent Herceptin(R) (trastuzumab) in metastatic breast cancer. a preliminary report. *Eur J Cancer* **37 Suppl 1**, 25-29 (2001).
46. Waldmann, T.A. Immunotherapy: past, present and future. *Nat Med* **9**, 269-277 (2003).
47. Doronina, S.O.*, et al.* Development of potent monoclonal antibody auristatin conjugates for cancer therapy. *Nat Biotechnol* **21**, 778-784 (2003).
48. Sakaguchi, S., Ishibashi, D. & Matsuda, H. Antibody-based immunotherapeutic attempts in experimental animal models of prion diseases. *Expert Opin Ther Pat* **19**, 907-917 (2009).
49. Zuber, C.*, et al.* Single chain Fv antibodies directed against the 37 kDa/67 kDa laminin receptor as therapeutic tools in prion diseases. *Mol Immunol* **45**, 144-151 (2008).
50. Hundt, C.*, et al.* Identification of interaction domains of the prion protein with its 37-kDa/67-kDa laminin receptor. *EMBO J* **20**, 5876-5886 (2001).
51. Deyev, S.M.*, et al.* Production of recombinant antitumor antibodies by HEK-293 cells. *Dokl Biochem Biophys* **406**, 44-46 (2006).
52. Durocher, Y., Perret, S. & Kamen, A. High-level and high-throughput recombinant protein production by transient transfection of suspension-growing human 293-EBNA1 cells. *Nucleic Acids Res* **30**, E9 (2002).
53. Thompson, E.W.*, et al.* The invasive and metastatic properties of hormone-independent but hormone-responsive variants of MCF-7 human breast cancer cells. *Clin Exp Metastasis* **11**, 15-26 (1993).
54. Wurm, F.M. Production of recombinant protein therapeutics in cultivated mammalian cells. *Nat Biotechnol* **22**, 1393-1398 (2004).
55. Kipriyanov, S.M. & Le Gall, F. Generation and production of engineered antibodies. *Mol Biotechnol* **26**, 39-60 (2004).

56. Ziober, B.L., Lin, C.S. & Kramer, R.H. Laminin-binding integrins in tumor progression and metastasis. *Semin Cancer Biol* **7**, 119-128 (1996).
57. Liotta, L.A.*, et al.* Metastatic potential correlates with enzymatic degradation of basement membrane collagen. *Nature* **284**, 67-68 (1980).
58. Campo, E.*, et al.* Detection of laminin receptor mRNA in human cancer cell lines and colorectal tissues by in situ hybridization. *Am J Pathol* **141**, 1073-1083 (1992).
59. Albini, A.*, et al.* A rapid in vitro assay for quantitating the invasive potential of tumor cells. *Cancer Res* **47**, 3239-3245 (1987).
60. Soule, H.D., Vazguez, J., Long, A., Albert, S. & Brennan, M. A human cell line from a pleural effusion derived from a breast carcinoma. *J Natl Cancer Inst* **51**, 1409-1416 (1973).
61. Osborne, C.K., Hobbs, K. & Clark, G.M. Effect of estrogens and antiestrogens on growth of human breast cancer cells in athymic nude mice. *Cancer Res* **45**, 584-590 (1985).
62. Albini, A.*, et al.* 17 beta-estradiol regulates and v-Ha-ras transfection constitutively enhances MCF7 breast cancer cell interactions with basement membrane. *Proc Natl Acad Sci U S A* **83**, 8182-8186 (1986).
63. Shafie, S.M. & Liotta, L.A. Formation of metastasis by human breast carcinoma cells (MCF-7) in nude mice. *Cancer Lett* **11**, 81-87 (1980).
64. Hughes, C.S., Postovit, L.M. & Lajoie, G.A. Matrigel: a complex protein mixture required for optimal growth of cell culture. *Proteomics* **10**, 1886-1890.
65. Vukicevic, S.*, et al.* Identification of multiple active growth factors in basement membrane Matrigel suggests caution in interpretation of cellular activity related to extracellular matrix components. *Exp Cell Res* **202**, 1-8 (1992).
66. Terranova, V.P.*, et al.* Use of a reconstituted basement membrane to measure cell invasiveness and select for highly invasive tumor cells. *Proc Natl Acad Sci U S A* **83**, 465-469 (1986).
67. Nogawa, M.*, et al.* Monitoring luciferase-labeled cancer cell growth and metastasis in different in vivo models. *Cancer Lett* **217**, 243-253 (2005).
68. Yano, J.*, et al.* Antitumor activity of small interfering RNA/cationic liposome complex in mouse models of cancer. *Clin Cancer Res* **10**, 7721-7726 (2004).
69. Hoffman, R.M. Orthotopic metastatic mouse models for anticancer drug discovery and evaluation: a bridge to the clinic. *Invest New Drugs* **17**, 343-359 (1999).

7. APPENDIX

APPENDIX A

Cell line data sheets:

HT-1080

DSMZ no.:	**ACC 315**
Species:	human (*Homo sapiens*)
Cell type:	fibrosarcoma
Origin:	established from the biopsy from a fibrosarcoma of a 35-year-old Caucasian man in 1972; patient did not receive any chemo- or radiotherapy
Depositor:	Dr. M. Wirth, GBF, Braunschweig, Germany
Biosafety:	Level 1

DSMZ Cell Culture Data:

Morphology:	epithelial-like adherent cells growing as monolayers
Medium:	90% Dulbecco's MEM + 10% h.i. FBS
Subculture:	split confluent culture about 1:10 every 3 days using trypsin/EDTA; seed out at ca. 1-2 x 10^6 cells/80 cm^2 + 7-10 ml medium
Incubation:	at 37 °C with 5-10% CO_2
Doubling time:	ca. 30 hours
Harvest:	cell harvest of ca. 25 x 10^6 cells/175 cm^2
Storage:	frozen with 70% medium, 20% FBS, 10% DMSO at about 1-2 x 10^6 cells/ampoule

DSMZ Scientific Data:

Mycoplasma:	negative in DAPI, microbiological culture, RNA hybridization, PCR assays
Immunology:	cytokeratin +, cytokeratin-7 -, cytokeratin-8 +, cytokeratin-17 -, cytokeratin-18 +, cytokeratin-19 -, desmin -, endothel -, EpCAM -, GFAP -, neurofilament -, vimentin +
Fingerprint:	multiplex PCR of minisatellite markers revealed a unique DNA profile
Species:	confirmed as human with IEF of AST, LDH, NP
Viruses:	ELISA: reverse transcriptase negative; PCR: EBV -, HBV -, HCV -, HHV-8 -, HIV -, HTLV-I/II , SMRV -

NIH/3T3

DSMZ no.: **ACC 59**
Species: murine (mouse, Swiss mouse) (*Mus musculus*)
Cell type: embryo
Origin: contact-inhibited NIH Swiss mouse embryo; used in DNA transfection assays
Depositor: Dr. H. Hauser, GBF, Braunschweig, Germany
Biosafety: level 1

DSMZ Cell Culture Data:

Morphology: fibroblast, adherent monolayer
Medium: 90% Dulbecco's MEM (4.5 g/L glucose) + 10% h.i. FBS (or NCS)
Subculture: do not allow culture to become completely confluent; split culture at 1:10 every 4 to 6 days using trypsin/EDTA; seed out at ca. 1 x 10^4 cells/cm^2
Incubation: at 37 °C with 5-10% CO_2
Doubling time: ca. 20 hours
Harvest: cell harvest of about 8 x 10^4 cells/cm^2
Storage: frozen with 70% medium, 20% FBS, 10% DMSO at about 0.7 x 10^6 cells/ampoule

DSMZ Scientific Data:

Mycoplasma: contamination was eliminated with Mycoplasma Removal Agent, then negative in DAPI, microbiological culture, RNA hybridization, PCR assays
Species: confirmed as mouse with IEF of AST, MDH, PEP B and by species PCR
Viruses: ELISA: reverse transcriptase negative; PCR: SMRV –

SW480

DSMZ no.: **ACC 313**
Species: human (*Homo sapiens*)
Cell type: colon adenocarcinoma
Origin: established from the tumor of a 50-year-old Caucasian man with colon adenocarcinoma (grade 4, Duke class B)
Depositor: Dr. H. Kirchner, Medical School Hannover, Hannover, Germany
Biosafety: level 1

DSMZ Cell Culture Data:

Morphology: endothelial-like adherent cells, mostly bipolar with microvilli growing in monolayers
Medium: 90-95% RPMI 1640 + 5-10% h.i. FBS
Subculture: split confluent culture 1:5 to 1:10 once a week using trypsin/EDTA; seed out at about 1.0 x 10^6 cells/80 cm^2; an 80 cm^2 culture flask becomes confluent within 1 week
Incubation: at 37 °C with 5% CO_2
Doubling time: 25-30 hours
Harvest: cell harvest of about 10-15 x 10^6 cells/80 cm^2
Storage: frozen with 70% medium, 20% FBS, 10% DMSO at about 3 x 10^6 cells/ampoule

DSMZ Scientific Data:

Mycoplasma: negative in DAPI, microbiological culture, RNA hybridization, PCR assays
Immunology: cytokeratin +, cytokeratin-7 -, cytokeratin-8 +, cytokeratin-17 -, cytokeratin-18 +, cytokeratin-19 +, desmin -, endothel -, EpCAM +, GFAP -, neurofilament -, vimentin +
Fingerprint: multiplex PCR of minisatellite markers revealed a unique DNA profile
Species: confirmed as human with IEF of AST, LDH, MDH
Viruses: ELISA: reverse transcriptase negative; PCR: EBV -, HBV -, HCV -, HIV -, HTLV-I/II -, SMRV –

HeLa

DSMZ no.: **ACC 57**

Species: human (*Homo sapiens*)

Cell type: cervix carcinoma

Origin: established from the epitheloid cervix carcinoma of a 31-year-old black woman in 1951; later diagnosis changed to adenocarcinoma; first aneuploid, continuously cultured human cell line

Depositor: obtained from ATCC (CCL 2), Rockville, Maryland, USA

Biosafety: level 1

Risk assessment: The cell line is infected with papilloma virus type 18 (HPV-18). An activation and transmission of the HPV-18 during handling of the cell line is improbable. The cell line is categorized biosafety level 1.

DSMZ Cell Culture Data:

Morphology: epithelial-like cells growing in monolayers

Medium: 90% MEM (with Earle's salts) + 10% h.i. FBS + 2 mM L-glutamine + non-essential amino acids (cells also grow well in 90-95% RPMI 1640 + 5-10% h.i. FBS)

Subculture: split confluent culture 1:4 to 1:6 every 3-5 days using trypsin/EDTA; cells reach confluence quickly; seed out at ca. 1-2 x 10^6 cells/80 cm^2

Incubation: at 37 °C with 5% CO_2

Doubling time: ca. 48 hours

Harvest: cell harvest of ca. 5-15 x 10^6 cells/175 cm^2

Storage: frozen with 70% medium, 20% FBS, 10% DMSO at about 1 x 10^6 cells/ampoule

DSMZ Scientific Data:

Mycoplasma: negative in DAPI, microbiological culture, RNA hybridization, PCR assays

Immunology: cytokeratin +, cytokeratin-7 +, cytokeratin-8 +, cytokeratin-17 +, cytokeratin-18 +, cytokeratin-19 +, desmin -, endothel -, EpCAM -, GFAP -, HMB-45 -, neurofilament -, vimentin +

Fingerprint: multiplex PCR of minisatellite markers revealed a unique DNA

Species: confirmed as human with IEF of G6PD, MDH, NP

Viruses: ELISA: reverse transcriptase negative; PCR: EBV -, HBV -, HCV -, HHV-8 -, HIV -, HPV +, HTLV-I/II -, SMRV -

LNCaP

DSMZ no.: **ACC 256**
Species: human (*Homo sapiens*)
Cell type: prostate carcinoma
Origin: established from the left supraclavicular lymph node metastasis from a 50-year-old man with prostate carcinoma in 1977; cells were described to be androgen-sensitive
Depositor: Prof. M. Motta, Universita di Milano, Milan, Italy
Biosafety: level 1

DSMZ Cell Culture Data:

Morphology: adherent fibroblastoid cells growing in aggregates and as single cells
Medium: 80% RPMI 1640 + 20% h.i. FBS
Subculture: split semi-confluent culture 1:4 once a week using trypsin/EDTA (occasionally cells can be detached by tapping); seed out at ca. 1-2 x 10^6 cells/25 cm^2; after thawing and trypsinization cells may need 1-2 days to become adherent again; due to the strong cell aggregation, it might be difficult to determine an exact cell titer
Incubation: at 37 °C with 5% CO_2
Doubling time: about 60 hours
Harvest: cell harvest of about 10-15 x 10^6 cells/80 cm^2 flask
Storage: frozen with 70% medium, 20% FBS, 10% DMSO at about 3 x 10^6 cells/ampoule

DSMZ Scientific Data:

Mycoplasma: negative in DAPI, microbiological culture, RNA hybridization, PCR assays
Immunology: cytokeratin +, cytokeratin-7 -, cytokeratin-8 +, cytokeratin-17 -, cytokeratin-18 +, cytokeratin-19 +, desmin -, endothel -, EpCAM +, GFAP -, neurofilament -, vimentin -
Fingerprint: multiplex PCR of minisatellite markers revealed a unique DNA profile
Species: confirmed as human with IEF of AST, MDH
Viruses: ELISA: reverse transcriptase negative; PCR: EBV -, HBV -, HCV -, HHV-8 -, HIV -, HTLV-I/II -, SMRV –

A-549

DSMZ no.: **ACC 107**

Species: human (*Homo sapiens*)

Cell type: lung carcinoma

Origin: established from an explanted lung tumor which was removed from a 58-year-old Caucasian man in 1972; cells were described to induce tumors in athmyic mice and to synthesize lecithin

Depositor: Dr. J. Wehland, GBF, Braunschweig, Germany

Biosafety: level 1

DSMZ Cell Culture Data:

Morphology: epithelial cells, growing adherently as monolayer

Medium: 90% Dulbecco's MEM + 10% h.i. FBS

Subculture: split confluent cultures 1:5 to 1:10 every 4-7 days using trypsin/EDTA; cells grow easily; seed out at ca. 1-2 x 10^6 cells/80 cm^2 + 10 ml medium

Incubation: at 37 °C with 5% CO_2

Doubling time: ca. 40 hours

Harvest: about 20 x 10^6 cells/175 cm^2

Storage: frozen with 70% medium, 20% FBS, 10% DMSO at about 0.5 x 10^6 cells/ampoule

DSMZ Scientific Data:

Mycoplasma: negative in DAPI, microbiological culture, RNA hybridization, PCR assays

Immunology: cytokeratin +, cytokeratin-7 +, cytokeratin-8 +, cytokeratin-17 -, cytokeratin-18 +, cytokeratin-19 -, desmin - , endothel - , EpCAM -, GFAP - , neurofilament - , vimentin +

Fingerprint: multiplex PCR of minisatellite markers revealed a unique DNA profile

Species: confirmed as human with IEF of MDH, NP

Viruses: ELISA: reverse transcriptase negative; PCR: EBV -, HBV -, HCV -, HHV-8 -, HIV -, HTLV-I/II -, SMRV –

MCF-7

DSMZ no.: **ACC 115**
Species: human (*Homo sapiens*)
Cell type: breast adenocarcinoma
Origin: established from the pleural effusion of a 69-year-old Caucasian woman with metastatic mammary carcinoma (after radio- and hormone therapy) in 1970; cells were described of being positive for cytoplasmic estrogen receptors and having the capability to form domes
Depositor: obtained from ATCC (HTB 22), Rockville, Maryland, USA
Biosafety: level 1

DSMZ Cell Culture Data:

Morphology: epithelial-like cells growing as monolayers
Medium: 90% RPMI 1640 + 10% h.i. FBS + MEM non-essential amino acids + 1 mM sodium pyruvate + 10 µg/ml human insulin
Subculture: split confluent culture 1:2 to 1:4 every 2-6 days using trypsin/EDTA; seed out at ca. 0.1-0.2 x 10^5 cells/cm^2
Incubation: at 37 °C with 5% CO_2
Doubling time: ca. 50 hours (range 30-72 hours)
Harvest: about 50-60 x 10^6 cells/175 cm^2
Storage: frozen with 70% medium, 20% FBS, 10% DMSO at about 0.8 x 10^6 cells/ampoule

DSMZ Scientific Data:

Mycoplasma: negative in DAPI, microbiological culture, RNA hybridization, PCR assays
Immunology: cytokeratin +, cytokeratin-7 -, cytokeratin-8 +, cytokeratin-17 -, cytokeratin-18 +, cytokeratin-19 +, desmin -, endothel -, EpCAM +, GFAP -, neurofilament -, vimentin -
Fingerprint: multiplex PCR of minisatellite markers revealed a unique DNA profile
Species: confirmed as human with IEF of AST, MDH
Viruses: ELISA: reverse transcriptase negative; PCR: EBV -, HBV -, HCV -, HHV-8 -, HIV -, HTLV-I/II -, SMRV –